CHARACTERIZATION OF HUMAN BABESIOSIS OTU LIKE PROTEIN

by
Betül Yusuf

Submitted to Graduate School of Natural and Applied Sciences
in Partial Fulfillment of the Requirements
for the Degree of Master of Science in
Biotechnology

Yeditepe University
2022

CHARACTERIZATION OF HUMAN BABESIOSIS OTU LIKE PROTEIN

APPROVED BY:

Assoc. Prof. Dr. Fatih Kocabaş ……
(Thesis Supervisor)
(Yeditepe University)

Assist. Prof. Dr. Hüseyin Çemin ……
(Yeditepe University)

Assist. Prof. Dr. Hilal Taymaz Nikerel ……
(Istanbul Bilgi University)

DATE OF APPROVAL: …./…./2022

I hereby declare that this thesis is my own work and that all information in this thesis has been obtained and presented in accordance with academic rules and ethical conduct. I have fully cited and referenced all material and results as required by these rules and conduct, and this thesis study does not contain any plagiarism. If any material used in the thesis requires copyright, the necessary permissions have been obtained. No material from this thesis has been used for the award of another degree.

I accept all kinds of legal liability that may arise in case contrary to these situations.

Name, Last name Betül Yusuf

Signature …..…….……..

ACKNOWLEDGEMENTS

I would like to give all my acknowledge and warmest thanks to my supervisor, Assoc. Prof. Dr. Fatih Kocabaş, for his invaluable supervision, made this work possible. His guidance and advice carried me through all the stages of writing my project. I appreciate my committee members for making my defense a positive experience and for their insightful comments and ideas.

My gratitude extends to the professors and doctors associated with succeeding in my Master's degree and the university administration, which had the most significant role in providing services and facilities to the students.

My lab mates and colleagues deserve to be acknowledged for their support, especially Sezer Akgol, for always being there for me, Birkan Girgin, Aynura Mammadova, Kardelen Tufekci, Delal Gulcin, Didem Aksu, Sumbul Yildrim, and Irem Buyuk for a cherished time spent together in the lab, and in social settings.

I would also like to give special thanks to my mom and dad and my family for their continuous support and understanding when doing my research and writing my project. Their prayers for me were what sustained me this far.

I would also thank my friends, especially Haya Alousi, for supporting and believing in me, Ferand Alhafiz, Salsabil Osama, Mahinur Mokhtar, and Saja Alyaacoub, and Rawan Mando for their support and warm friendship.

Finally, I would like to thank myself for the hard work and for being strong enough to go through all the ups and downs that I faced in the past years. I believe that the best is yet to come, and a new chapter has finally begun.

God is the arbiter of success.

ABSTRACT

CHARACTERIZATION OF HUMAN BABESIOSIS OTU LIKE PROTEIN

Babesia microti, a parasite that causes malaria-like symptoms, is the causative agent of Babesiosis, a protozoan parasite of red blood cells. Human Babesiosis can manifest on a spectrum of severity, ranging from being asymptomatic, and mild-to-moderate severity to being a severe illness that could result in death or incessant relapse. *B. microti* has increasingly gained resistance against therapeutic drugs. Other than the research mentioned earlier, targeting proteases necessary for the survival of B. microti can be possibly therapeutic, especially the ubiquitin proteasome pathway. The *Apicomplexan* pathogens that include *babesia microti* are intercellular parasites, and they are comparable to Crimean Congo Haemorrhagic Fever Virus (CCHFV). Several Viral OTU-related proteins were reported and showed that these proteins have the ability to alter the ubiquitination process and cleave the region of the ISG15 in the infected cells and it was proved that CCHFV has OTU de-ubiquitination activity when cells are invaded. In addition, the OTU deubiquitinase Y89-W99 pockets were determined as having a significant role in developing small molecule inhibitors for treating the diseases. *Babesia Microti*, an unnamed protein product, was predicted to be from the OTU-like cysteine protease. The results of the present study support the hypothesis that; if the CCHFV can use the deubiquitinase pocket to invade the cells, *babesia microti* (*B.microti*) OTU protein can also has the OTU de-ubiquitination activity since there are similarity between CCHFV and Viral OTU-like proteases. This is the first time that *babesia microti* OTU protein has been identified and characterized. The purpose of this study was to characterize the novel bm-OTU-like protein *in vitro* and *in vivo* and mainly its deubiquitination activity. The study represents the first direct demonstration of bm-OTU protease effects on the intracellular ubiquitination at the mono-poly-UB level and cellular immune pathways. Inhibition of this protease activity was planned in this study to develop new approaches for treating babesiosis disease. In conclusion, this study highlights the challenge of protein misfolding and deubiquitination activity of the bm-OTU recombinant protein *in vitro* and accredits any improvements in different conditions. It can be drawn from all the results shown in this study that the studied recombinant protein has been identified and characterized for any future work in order to develop any new approaches in the field of treatments.

ÖZET

İNSAN BABESİOZ OTU PROTEİN KARAKTERİZASYONU

Sıtma benzeri semptomlara neden olan bir parazit olan Babesia microti, kırmızı kan hücrelerinin bir protozoan paraziti olan Babesiosis'in etken ajanıdır. İnsan Babesiosis, asemptomatik ve hafif ila orta şiddette olmaktan ölüm veya sürekli nüksetme ile sonuçlanabilecek ciddi bir hastalık olmaya kadar değişen bir şiddet yelpazesinde kendini gösterebilir. B. microti, terapötik ilaçlara karşı giderek artan bir direnç kazanmıştır. B. microti'nin hayatta kalması için gerekli proteazları hedeflemek, özellikle ubikuitin proteazom yolunu hedeflemek muhtemelen terapötik bir yaklaşım olabilir. Babesia microti'yi içeren Apicomplexan patojenleri hücreler arası parazitlerdir ve Kırım Kongo Kanamalı Ateş Virüsü (CCHFV) ile karşılaştırılabilir özelliklere sahiptir. Birkaç Viral OTU ile ilgili protein rapor edilmiştir ve bu proteinlerin, ubiquitination sürecini değiştirme ve enfekte olmuş hücrelerde ISG15 bölgesini parçalama yeteneğine sahip olduğunu gösterilmiştir ve hücreler istila edildiğinde CCHFV'nin OTU de-ubiquitination aktivitesine sahip olduğu kanıtlanmıştır. Ek olarak, OTU deubiquitinase Y89-W99 ceplerinin, hastalıkların tedavisi için küçük molekül inhibitörlerinin geliştirilmesinde önemli bir role sahip olduğu belirlendi. Bilinmeyen bir protein ürünü olan Babesia Microti'nin OTU benzeri sistein proteazından olduğu belirledik. Mevcut çalışmanın sonuçları şu hipotezi desteklemektedir; CCHFV, hücreleri istila etmek için deubikuitinaz cebini kullanabilirse, babesia microti (B.microti) OTU proteini, CCHFV ve Viral OTU benzeri proteazlar arasında benzerlik olduğundan, OTU de-ubiquitination aktivitesine de sahip olabilir. Bu çalışmada, babesia microti OTU proteininin ilk kez tanımlanması ve karakterize edilmesi hedeflenmiştir. Bu çalışmanın amacı, yeni bm-OTU benzeri proteini in vitro ve in vivo ve esas olarak deubikitinasyon aktivitesini karakterize etmekti. Çalışma, mono-poli-UB seviyesinde hücre içi çoğalma ve hücresel bağışıklık yollarında bm-OTU proteaz etkilerinin ilk doğrudan gösterimini temsil etmektedir. Babesiosis hastalığının tedavisi için yeni yaklaşımlar geliştirmek için bu çalışmada bu proteaz aktivitesinin inhibisyonu planlandı. Sonuç olarak, bu çalışma, bm-OTU rekombinant proteininin in vitro olarak protein yanlış katlanması ve deubiquitination aktivitesinin zorluğunu vurgulayan sonuçlara ulaşılmıştır ve yapılması gereken çalışmaların gereğini ortaya koymuştur.

TABLE OF CONTENTS

LIST OF FIGURES

LIST OF TABLES

LIST OF SYMBOLS/ABBREVIATIONS

AMC	7-amino-4-methyl coumarin
BCA	Bicinchoninic acid assay
bm	Babesia Microti
CCHF	Crimean-Congo haemorrhagic fever
CCHFV	Crimean-Congo haemorrhagic fever virus
DMEM	Dulbecco's Modified Eagle Medium
DMSO	Dimethyl sulfoxide
DUB	Deubiquitinase
GFP	Green fluorescent protein
HEK293T	Human embryonic kidney 293 with the SV40 large T antigen
IPTG	Isopropyl ß-D-1-thiogalactopyranoside
kDa	Kilo Dalton
LB	Luria Bertani
mg	Milligram
mL	Milliliter
µg	Microgram
µl	Microliter
OTU	Ovarian tumor unit domain
PBS	phosphate buffered saline
PCR	Polymerase chain reaction
PEI	polycation polyethylenimine
PVDF	Polyvinylidene fluoride
RBCs	Red blood cells
rpm	Revolutions per minute
SDS-PAGE	Sodium dodecyl sulfate–polyacrylamide gel electrophoresis
TBS	Tris-buffered saline
TBST	Tris-buffered saline with Tween® 20 detergent
Ub-AMC	Ubiquitin-7-amino-4-methyl coumarin

1. INTRODUCTION

1.1. HUMAN BABESIOSIS AND TICK-BORNE PATHOGENS

Tick-borne infections can be transmitted to people through the biting of ticks that are infected. Ticks can carry germs, viruses, and parasites, among other things. Tick-borne diseases such as Babesiosis, Southern Tick-Associated Rash Illness, Tick-Borne Relapsing Fever, and tularemia are the most frequent in the United States. Colorado tick fever, Powassan encephalitis, and fever are among the tick-borne diseases found in the United States. It is the most widely described tick-borne disease, with Lyme disease being the most common. Over 22,500 confirmed cases of Lyme disease and 7,500 suspected cases of Lyme disease were documented towards the Centers for Disease Control and Prevention (CDC) in 2010 [1].

On the other hand, Babesiosis is serious and potentially life. It is caused mainly through the intraerythrocytic protozoan *Babesia microti*, which is an emerging zoonotic disease. It is indeed endemic to the northeastern as well as upper midwestern United States, where it is transferred most frequently through the black-legged tick, Ixodes scapularis, which is also the causative agent for Lyme disease as well as anaplasmosis [2]. Human Babesiosis can develop as a clinical spectrum starting from an influenza-like illness (characterized by sore head, fever, chills, nausea, vomiting, and myalgia) to the type of fulminant multi-organ failure seen with falciparum malaria, which is associated with a high fatality rate [3]. It is not unexpected that human Babesiosis is frequently misrecognized as falciparum malaria, given that the latter's more severe pathology (which is most widely seen in splenectomized individuals) such as altered mental status, disseminated intravascular coagulation, anemia with dyserythropoietic, hypoxemia, adult respiratory failure syndrome, and renal insufficiency [4].

Babesia microti, a parasite that causes malaria-like symptoms, is the causative agent of Babesiosis, a protozoan parasite of red blood cells. *B. microti* is spread by Ixodes dammini nymphs, which are also the principal vector of Lyme disease in the northeastern United States. *Peromyscus leucopus* (white-footed mice) and *Microtus pennsylvanicus* (meadow voles) are carriers for both *Borrelia microti* and *Borrelia burgdorferi,* that is the causative

agent of Lyme disease [5]. Babesiosis and Lyme disease were observed to coexist in humans [6].

1.2. HISTORY OF THE INFECTIOUS DISEASE

Babesiosis disease is caused by intraerythrocytic protozoans that can be introduced by ticks via blood transfusion or transplacentally. Babesiosis First noticed by Victor Babes in 1888, the babesia microorganisms are now identified as the cause of hemoglobinuria in cattle [7]. The first was described as a clinical entity in 1888 when Babes was researching the deaths of up to 50,000 cows in Romania; Babes named the disease Babesia. Anemia, fever, and hemoglobinuria were the first symptoms documented by Smith and Kilborne in their 1893 description of the disease as a tick-borne illness in cattle [8].

In 1908, Wilson and Chowning found illegitimately intraerythrocytic inclusions similar to those described by Smith and Kilbourne in the blood of Rocky Mountain spotted fever patients in the western United States. *Phytoplasma hominins* were the name given to this pathogen. When a Yugoslav farmer was diagnosed with Babesiosis, it was the first time the disease had been proven in humans [6]. Even though the first case was reported in California in 1966, it has never been confirmed which type of Babesia is responsible for this infection. *Babesia microti* is the first documented human infection that occurred on Nantucket Island, Massachusetts, in 1969 [9,10]. Infections with *B. microti* were generally documented in towns along the coasts of Connecticut, Massachusetts, New York, and Rhode Island since it was first discovered on an offshore island in New England, and the disease has since migrated to the interior of the state [11]. In fact, since 1969, hundreds of instances of human Babesiosis were detected in the United States, with an increasing frequency each year after the first case was reported [12].

Since 1982, more than 200 human cases of Babesiosis have been stated in the eastern US, providing the declaration of formulating Babesiosis as a reportable disease in some states, including New York [13]. Babesiosis is most commonly brought on by B. microti in North America [14]. However, in Europe, about 50 cases have been documented since the 1950s [15]. The *Ixodes ricinus* tick is widely recognized as the primary human disease vector, and it has been shown to transmit at least *B. divergens* and *B. microti* to humans. In Poland, only one asymptomatic case was reported [16].

B. microti infection is most commonly acquired through blood transfusions in Europe, resulting in the most severe cases. Babesiosis is primarily transmitted by ticks in the world, including in Japan, China, the Asia-Pacific area, and Australia, as well as the United States [17,18]. Also France and the British Isles were reported for more than half of all cases in Europe. Many additional European nations have seen proven cases of the disease in the recent decade: Austria; Czech Republic; Finland; Germany; Italy; Montenegro; Portugal; Poland; and Switzerland [15]. Europe looks to be the least affected region in the world by human Babesiosis compared to the United States. However, it appears to be the most severe [14,19].

1.3. DATA AND STATISTICS OF HUMAN BABESIOSIS IN THE WORLD

There have been reports of human Babesiosis in 28 countries across all continents. Except for the United States of America, Canada, China, and France, all countries have less than ten documented incidents and will be addressed in further detail. As a result of this current emergence of human Babesiosis caused primarily by B. microti, the United States of America and Canada, both of which are located in North America, account for more than 95 percent of all recorded cases worldwide and are thus considered "ground zero" of the current global outbreak (Figure 1.1.).

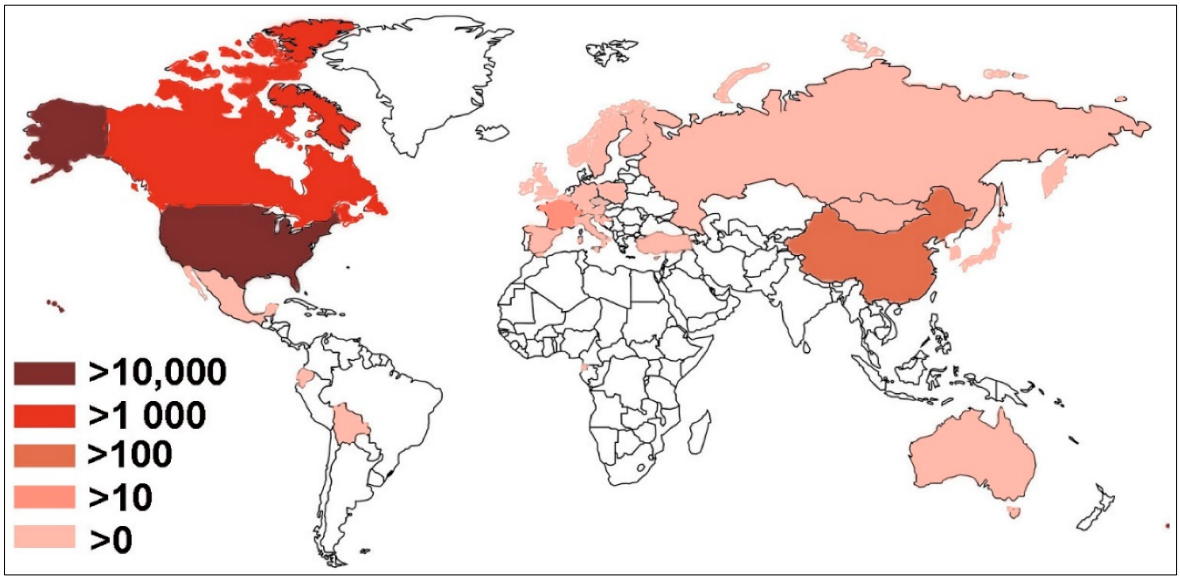

Figure 1.1. Human Babesiosis distribution in the world [20]

Since January 2011, human Babesiosis has been classified as a notifiable disease in the United States [2,20]. Due to the lack of reporting and misdiagnosis, this figure is believed to be an underestimate of the total number of infections [21]. Transfusion-transmitted Babesiosis can occur year-round, even in locations where the disease is not endemic, despite most cases occurring during or shortly after the summer in areas where the disease is endemic. About one in five incidents of blood transfusion-related deaths have been fatal [22]. In 2019, (CDC) was informed of 2,418 cases of Babesiosis in 25 of the 40 states where Babesiosis was an actual condition at 63 percent [2]. Since the first European case of human Babesiosis was recorded in the late 1950s, more than 60 others have been discovered across Europe [23].

Several other European nations, including Austria, Finland, Germany, Italy, Portugal, and Switzerland, have reported confirmed cases of the disease in the last decade [15]. There have been 29 cases of human Babesiosis documented, particularly in France, and the British Isles represented almost more than half of those cases [24]. They were also found in Spain, Sweden, Switzerland, Belgium, and Russia, and two asymptomatic cases of B.microti infections in Poland [25-29]. However, it is difficult to provide an accurate representation of the epidemiology of Babesiosis in Europe due to the fact that symptoms might be unclear or non-specific in immunocompetent patients [30].

1.4. HUMAN BABESIOSIS DESCRIPTIVE CLINICAL AND EPIDEMIOLOGICAL INFORMATION

Holoparasites, or obligate parasites, are organisms that require the exploitation of a host in order to complete their life cycle. As the name suggests, the reproduction of obligate parasites is fully dependent on obtaining a host. Obligate parasites use several strategies to obtain and exploit the host. These parasites often preserve the health of the host since the host provides parasites with nutrition and reproductive needs, except when host death is needed for transmission. Many organisms exhibit obligate parasitism, including viruses, some bacteria, fungi, and animals. Some parasites are ectoparasites, exploiting hosts by attaching to their epidermis, or endoparasites, exploiting the host internally. Other parasites are called brood parasites. They do not attach directly to the host but rather infest eggs or spores onto the host from a distance [31].

Human Babesiosis is an infectious disease caused by *Babesia* protozoa, which are obligate intracellular endoparasites that exploit red blood cells. *Babesia* has been previously known to infect animals, but during the past 50 years, the parasite has increasingly infected humans as well. Babesiosis is tick-borne, meaning that the parasite can be transferred to humans through the tick intermediary. The first scientist to document the disease was Viktor Babes, who studied febrile hemoglobinuria (abnormal transportation of oxygen in hemoglobin due to the destruction of red blood cells [32]) in Romanian sheep. He reported the presence of a protozoan organism in cattle red blood cells and named it *Babesia bigemina* [33]. Later on, the first human case reported was in 1957 in Croatia, where a farmer developed a fever accompanied by hemoglobinuria and anemia after herding tick-infested cattle [34].

1.4.1. Epidemiology

Babesiosis epidemiology depends on several factors like host availability, the presence of an infected tick vector, as well as favorable conditions for transmission. The absence of any of these parameters ceases infection transmission [35].

1.4.2. Pathogen

Babesia species are all part of the Apicomplexa phylum. Babesia shares this phylum with malaria-causing Plasmodia and toxoplasmosis-causing Toxoplasma gondii. Organisms of the Apicomplexa phylum are all distinct in their special organelle called the apical complex during some cellular stages in the organism's development. These unique organelles allow organisms from the Apicomplexa phylum to penetrate potential host cells by secreting enzymes. The enzyme-secreting complex comprises micronemes, conoid, rhoptries, and polar rings [36], as shown in Figure 1.2.

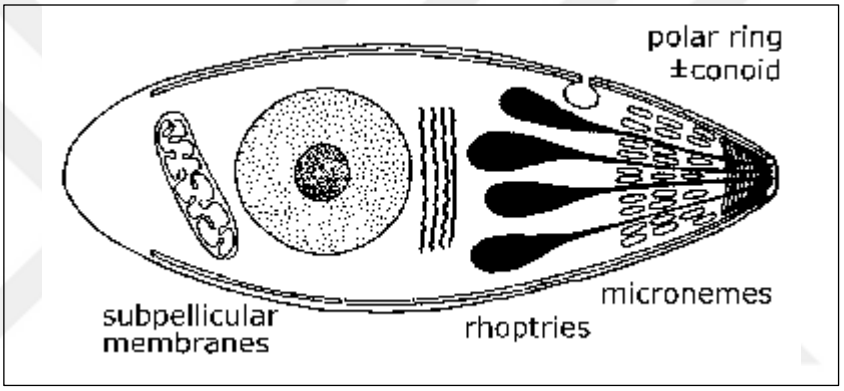

Figure 1.2. Apical Complex in Apicomplexans [5]

The life cycle of *Babesia* species involves reproduction in two separate hosts: asexually in mammalian blood cells and sexually in arthropods, most commonly ticks. In erythrocytic reproduction, *Babesia* progeny lyse erythrocytes as they egress, latching onto other blood cells and continuing their asexual reproduction. Ticks that ingest infected blood also take in the Babesia parasite, which permeates the epithelium of tick guts [37].

1.4.3. Transmission

The most common parasite causing human babesiosis disease is Babesia microti, which infests itself in Ixodes scapularis deer ticks. In the US, Peromyscus leucopus, or the white-footed mouse, holds the biggest reservoir of B. microti [38]. Since ticks require a blood meal in order to mature from each stage of their life cycle to the next (larva to nymph to adult), the transmission starts when tick larvae hatch in spring. Later in the summer, the larvae feed

on a blood meal from a rodent infected with B. microti. After the blood meal, larvae are able to develop into nymphs and transmit Babesia to other rodents. Ticks, in all their life stages, can feed on humans as well as deer, but nymphs have been reported to be the main proprietor of Babesia [39]. A 1989 study correlated the surge in deer population to the increase in human Babesiosis [40]. The transmission rate of human Babesiosis due to blood or transplacental transfusions is low. Figure 1.3. describes the transmission of Babesia as described above.

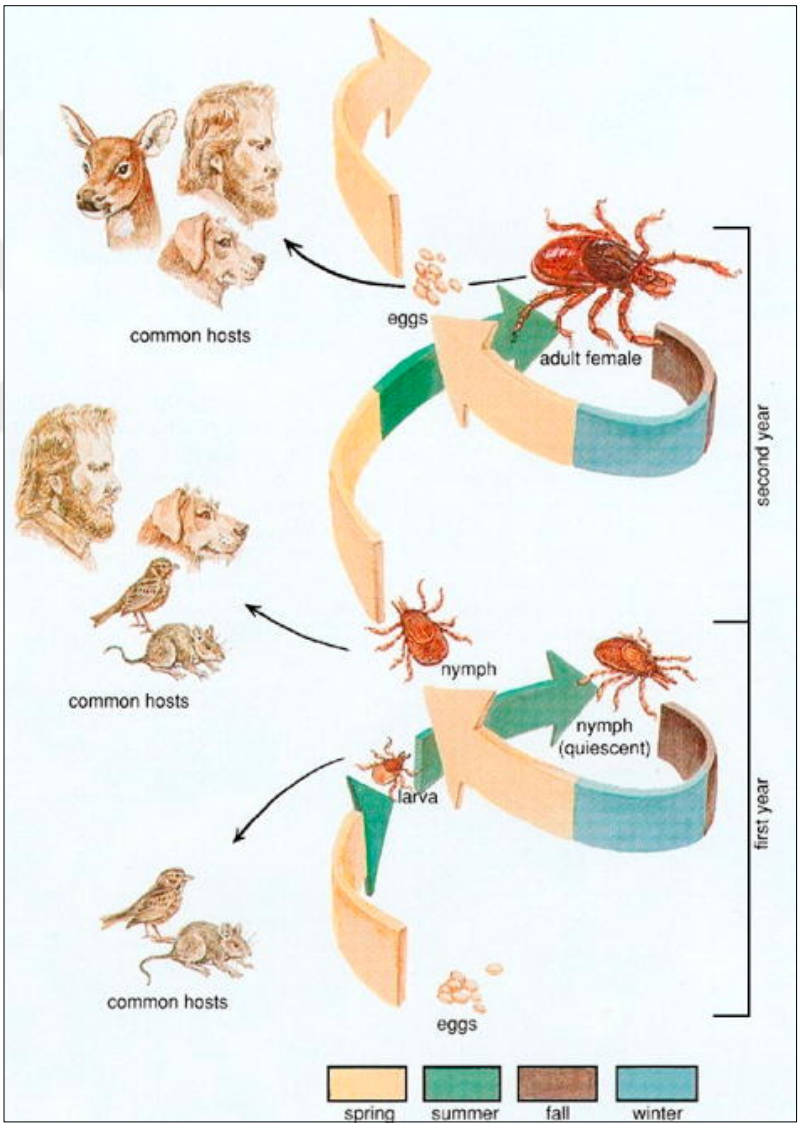

Figure 1.3. Babesia Transmission Through Different Hosts Annually [39]

1.4.4. Human Epidemiology

As previously mentioned, the past 50 years exhibited a change from having the human babesiosis disease in a few isolated cases around the world to being an endemic disease in US areas like the northern central Midwest and New York. In the US, human Babesiosis is prevalently caused by *B. duncani*, while *B. microti* is shown to be the main cause of the disease in Europe and Asia [41]. Most human babesiosis cases manifest themselves during the summer, especially in regions where deer, rodents, and ticks are relatively close to humans, especially children [42].

1.5. CLINICAL MANIFESTATIONS

Human Babesiosis can manifest on a spectrum of severity, ranging from being asymptomatic, mild-to-moderate severity to being a severe illness that could result in death or incessant relapse. Symptoms of babesia disease start showing on humans about 1-6 weeks from a tick bite.

1.5.1. Mild-Moderate Illness

Most babesiosis patients experience mild symptoms that are regarded as discomfort, fatigue, fever, sweats, anorexia, and myalgia (muscle pain). Some patients also exhibit nausea, vomiting, depression, and emotional distress. Upon physical examination, minimal symptoms can be found, excluding fever. Some patients with mild illness are clinically present with an enlarged spleen or liver and jaundice, retinopathy (eye dysfunction). In mild illness, symptoms last weeks up to months, with a recovery that lasts for a year. After symptom recovery, *Babesia* may still exist in the human body, causing an asymptomatic infection [43].

1.5.2. Severe Illness

People who have a suppressed or jeopardized immunity are more susceptible to a more severe illness upon infection with *Babesia microti.* Having an immune disease like HIV or

taking immunosuppressants weakens the human immune defense system against infections that would otherwise be contained and fought. Moreover, people who are over 50 years old are also more likely to showcase severe symptoms of Babesiosis [44]. Generally, Babesiosis caused by *B. microti* is less severe than that caused by *B. duncani* or *B. divergens* [45].

Severe complications of human Babesiosis can include respiratory, heart, renal, and liver failure, as well as splenic infarction. The most common severe symptom among patients is acute respiratory failure, with a mortality rate of 5 percent when infected with *B. microti* [46].

1.5.3. Asymptomatic Illness

Most patients with asymptomatic Babesiosis acquire infection through the bite of an infected tick. Asymptomatic Babesiosis continues for months up to years after all illness symptoms resolve. About one-third of babesiosis patients are asymptomatic. Asymptomatic parasitemia is more common in children between 4 and 10 years of age. The long asymptomatic period in human hosts increases *B. microti* transmission rate to other hosts [42].

1.6. BABESIA MICROTI

1.6.1. Morphology

B. microti belongs to one of two morphological groups of the babesia genus. Small babesias, which include *B. microti*, are between 1 and 2.5 micrometers long. Small babesias form obtuse angles to each other in red blood cells as it seen in Figure 1.4.

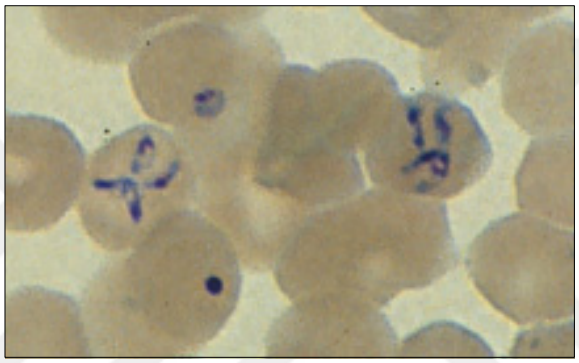

Figure 1.4. Morphology of B. microti in Erythrocytes [38]

1.6.2. Life Cycle

As mentioned before, the life cycle of *B. microti* involves the presence of two hosts, a rodent and a tick. Infected ticks transmit babesia sporozoites to a mouse host during their blood meal. Sporozoites undergo asexual reproduction in red blood erythrocytes of the mouse via the process of budding, forming gametes. During the second blood meal, ticks ingest babesia gametes, where gametes fuse and start producing more sporozoites via their sporogenic cycle. When humans are bitten by infected ticks, humans act as the rodent host, where they hold sporozoites that reproduce in RBCs. This reproduction is what causes clinical presentation and symptoms since babesia burst RBCs as they transmit themselves within the human body. Humans rarely transmit B microti to other ticks during another blood meal, so they are considered a dead-end for the babesia life cycle [47].

1.6.3. Phylogenetic Tree

B. microti is an apicomplexan of the clade Hematozoa, the same clade that includes parasites that infect hemocytes of vertebrates. Hematozoa clade is divided into two major groups, the Haemosporidia and Piroplasmidia.

The Babesia genus belongs to the Piroplasmidia clade. As previously described, they have a definite invertebrate host and an intermediate vertebrate host. As it seen in Figure 1.5. phylogenetic analysis shows that ancestors of the Hematozoa clade may have been a photosynthetic ancestor that is flaggelated and has cortical alveoli [48].

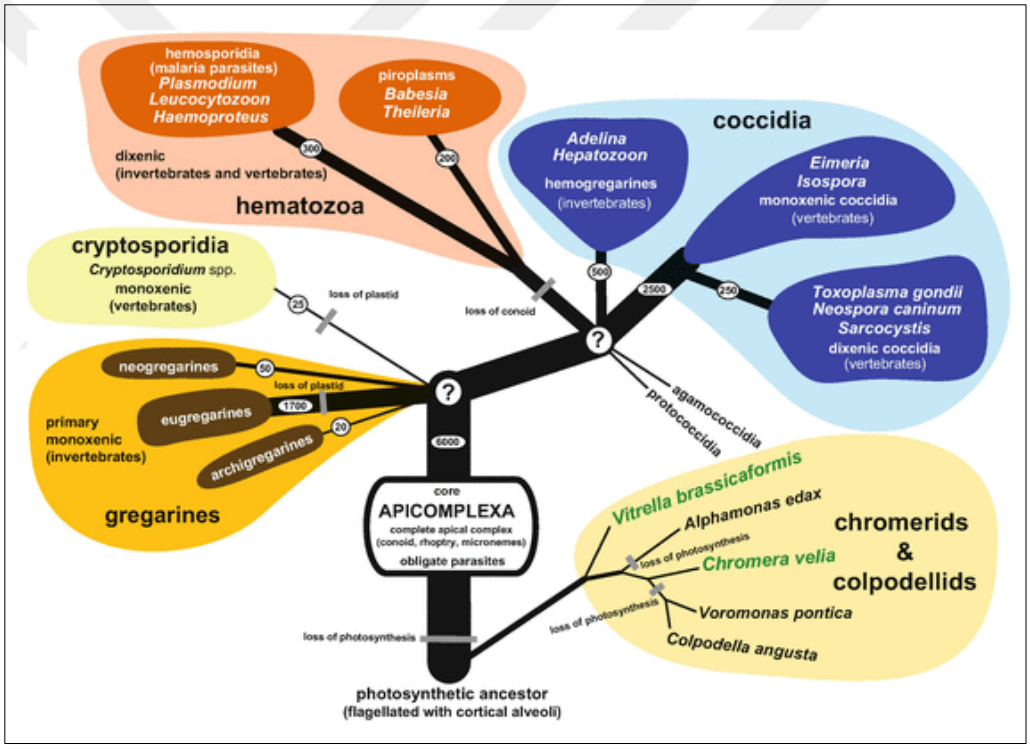

Figure 1.5. Phylogenetic Tree of Babesia [48]

1.7. PATHOGENESIS

The pathogenesis of human Babesiosis occurs through two processes, medication of RBCs and the human immune system response.

1.7.1. Modification of RBCs

Human infection with B. microti only affects erythrocytes, which are the oxygen-carrying red blood cells. Babesia latches onto erythrocytes via surface antigens on RBCs called VMSAs. Moreover, sialo-glycoproteins and glycosaminoglycans on RBCs help in mediating the attachment. After babesia gametes are oriented favorably for successful attachment, the conical apex that characterizes Babesia starts secreting proteins that allow them to perforate RBCs and enter them. Inside erythrocytes, Babesia reproduces via fission or budding, each of which can form up to 4 progeny called "merozoites". After reproduction and incubation, babesia burst opens the RBCs and transmit themselves to other erythrocytes within the human body. This can therefore cause anemia and/or hypoxia since RBCs are responsible for the delivery of oxygen to organ tissues [49].

One of the proteins secreted by Babesia in order to enter RBCs is called VESA1 (*variant erythrocyte antigen 1*). The gene which encodes this protein has been studied to be highly polymorphic, meaning that there are many different variations of the gene encoding the protein. These variations are exactly what allow Babesia to evade the human immune response. VESA1 has been shown to urge red blood cells to adhere to the endothelium of vascular tissue. Adherence to vascular tissue is advantageous for babesia infection since it decreases access of immune cells to infected RBCs. Also, it blocks the removal of the affected RBCs to the spleen [50].

1.7.2. Immune Response

The human immune response is always ready to fight off any infection, including that of Babesia. The immune system works via secreted cytokines and chemokines, causing an inflammatory response, which calls onto the white blood cells to fight off the infection. Studies done on mice infected with B. duncani showed that IFN-gamma cytokine is vital for survival [51]. Moreover, the same cytokine in mice infected with B. microti is shown to prevent the immune response against the parasite [52].

This difference is due to the different immune cells in action against each infection. Mice use CD4+ cells in the immune response against B. duncani and NK cells against B. microti. The cytokine IFN-gamma is secreted along with other cytokines to urge an inflammatory

response to activate macrophages that kill the parasites via nitric acid secretions. Inflammation is maintained at a certain localization via the fine-tuning of inflammatory and anti-inflammatory cytokines [53].

It is intuitive to think that a stronger infection requires a stronger immune response. But this could, in fact, be dangerous since the inflammation could spread to vital organs and cause the body to be in a state of sepsis. As mentioned earlier, respiratory distress is one of the most common symptoms of human Babesiosis. The main reason for this symptom is excess cytokine release [54].

1.8. OTU-PROTEIN AND BABESIA MICROTI AS AN INTRACELLULAR PARASITE

Numerous human and animal illnesses are caused by nairoviruses. For example, Crimean Congo hemorrhagic fever virus (CCHFV), a research has linked the viral ovarian tumor domain (vOTU) to nairovirus virulence because of its ability to edit ubiquitin (Ub) bound to cellular proteins and to break down the Ub-like protein interferon-stimulated ISG15 that has improtant role in protein stability [55]. The deubiquitinase of the OTU family encoded by CCHFV and related viruses, and targeted ISG15 alterations [56,57]. CCHFV ovarian tumor protein is able to antagonize NF-κB signaling which is critical to viral invasion [58]. It has been recognized a cysteine viral ovarian tomur domain protease in the CCHFV protein. More than 100 eukaryotic and viral proteins have been classified in the OTU superfamily members [(59,60)]. A viral OTU like deubiquitinase was determined compared to CCHFV OTU deubiquitinase which has the ability to perform intracelluar invasion by using deubiquitinzation activity [61]. In fact, the babesia microti OTU protein was predected to be an OTU-Like protein, which causes babesiosis disease, using bioinformatic approaches [62,63]. Interestingly, this OTU-Like protein has not been identified yet.

1.9. DETECTION AND DIAGNOSIS OF THE BABESIOSIS DISEASE

Upon the presentation and diagnosis of a patient with Babesiosis, it is important to make sure that even with the presence of all symptoms matching Babesiosis, definitive detection is required for proper diagnosis. Microscopy is the go-to method of detection and diagnosis

after staining blood smears with Giemsa dye. Moreover, molecular methods can be used for more rapid and accurate detection. A vertical flow visualization strip can be used for this purpose [55]. Furthermore, PCR and DNA sequencing can also be performed to compare patient sequencing to a known database of babesia sequences [56].

1.9.1. Clinical Diagnosis

Clinically, a diagnosis surely depends on the presence of symptoms that match that of Babesiosis covered above. However, it could get tricky since these symptoms overlap many symptoms of other diseases as well. So the key lies in differentiating between Babesiosis and other illnesses. A physician is not able to diagnose Babesiosis merely from a physical exam. Nonetheless, Babesiosis should be on the list of diseases when the patient presents with viral-like symptoms and has spent time in tick-infested areas during summer or spring. Patients of human granulocytic anaplasmosis and Lyme disease are also highly likely to have contracted Babesiosis since any combination of these three diseases can be spread via the tick *I. scapularis*. To certify babesiosis diagnosis, a lab workup must be performed after a blood transfusion [57].

1.9.2. Laboratory Diagnosis

The main pointer for a babesiosis infection is the diminishing in RBC count in sick patients. Indications of RBC lysis include hyperbilirubinemia (buildup of bilirubin in the blood causing jaundice), hemolytic anemia, elevated indirect bilirubin fraction, elevated LDH, and decreased haptoglobin levels. Moreover, a urinalysis can reflect hemolysis. However, all these indications are non-definitive.

A definitive diagnosis can be made with microscopy after staining blood smears with a dye. Babesia can be then seen as round or pear-shaped dots, with the cytoplasm dyed blue and chromatin dyed red. The distinguishing characteristic of Babesia is that some extra-erythrocytic forms can be seen in severe cases. Moreover, the presence of merozoite tetrads, or the "Maltese Cross", is definitive of Babesiosis.

If blood smears show negative results and Babesiosis is still highly suspected, a PCR test can be performed to test for the babesia genome in the blood. PCR tests are sensitive and accurate. Also, the blood can be screened for anti-babesia immunoglobulins via an immunofluorescence assay.

Lastly, if all tests fail, the only remaining solution is to inject a sick patient's blood into hamsters since they have a relatively quick incubation rate and are very susceptible to Babesiosis. Parasitemia would develop within 2-4 weeks.

1.10. TREATMENT OF THE BABESIOSIS DISEASE

Treatment should start right after the definitive diagnosis of Babesiosis. The most common treatment includes antimicrobial combinations, most commonly: atovaquone & azithromycin and clindamycin & quinine [67].

1.10.1. Mild Infection

Mild to moderate Babesiosis can be treated by administering the atovaquone + azithromycin combination for 7-10 days. An alternative is the clindamycin + quinine combination; however, serious side effects can occur with the use of this combination. In a study by Krause *et. al,* 15 percent and 72 percent of subjects with Babesiosis who were treated with atovaquone + azithromycin and clindamycin + quinine, respectively, suffered serious side effects [68]. Atovaquone + azithromycin combination has also shown successful treatment in children. In conclusion, atovaquone + azithromycin antimicrobial combination is preferred in mild cases.

1.10.2. Severe Infection

For patients with severe illness, the clindamycin + quinine antimicrobial combination administered over 7-10 days is the preferred treatment for B. microti babesiosis [68]. This medication should be following a blood transfusion since patients with severe cases (more than 10 percent parasitemia) have compromised oxygenation and RBC count. Exchange RBC blood transfusion is also vital in cases of pulmonary, hepatic, or renal failure (the

adverse effects of tissue hypoxia). In this case, the exchange in RBCs removes some of the burdens on antimicrobial medication and removes babesial toxins from the blood.

1.10.3. Asymptomatic Infection

Patients with asymptomatic Babesiosis are not treated, even with a definitive diagnosis, unless their parasitemia lasts for over three months. Moreover, patients with a discovered immunity against Babesia (presence of anti-babesial immunoglobulins) but with negative blood smears. Such patients are likely to have contracted Babesiosis, and their bodies resolved it on their own. Since Babesiosis may continue to manifest itself asymptomatically after being symptomatic, immunocompromised patients should get several blood smears every few months until Babesia clears their system completely [69].

1.11. THE CHALLENGES OF IMPLEMENTING A BABESIOSIS MEDICINE

As previously mentioned, immunocompromised patients may still have a persistent infection even after administering the treatments above. One study showed that the atovaquone-proguanil combination eradicated Babesia from an immunocompromised babesiosis patient [70]. However, in another study of 14 very immunocompromised babesiosis patients, none of the subjects were successfully treated with any antimicrobial combination [71]. Nonetheless, a cure was found with progressive treatment for six weeks, being maintained for two weeks after the last babesia-free blood smear.

Therefore, the biggest challenge of finding a babesiosis medicine lies in the ambiguity of patient response to the medications suggested. Finding and fine-tuning the antimicrobial combinations is crucial, especially for immunocompromised patients. Future treatments are currently under study, aiming at studying the role of humoral immunity in fighting off Babesiosis. Passive immunotherapy with intravenous immunoglobulin injection or subcutaneous IFN-gamma administration may help immunocompromised babesiosis patients [71].

B. microti has increasingly gained resistance against therapeutic drugs. Other than the research mentioned earlier, targeting proteases necessary for the survival of B. microti can be possibly therapeutic, especially the ubiquitin proteosome pathway [72].

1.12. UBIQUITIN PROTEASOME PATHWAY

The ubiquitin proteosome pathway (UPP) is essential for babesial survival because it has an essential role in the destruction of dysfunctional proteins through the proteosome and protease enzymes. This pathway maintains the quality of proteins in organisms. Defective ubiquitin proteasomes disturb the cellular balance and may be fatal for the organism.

Since the UPP regulates the protein content in organisms destructively, UPP regulation is called a *negative* regulation. Only proteins marked by the 76-aminoacid ubiquitin post-translationally are marked for proteasomal destruction. 26S unit of proteosomes recognizes ubiquitin [73].

The UPP consists of three main processes: ubiquitination, recognition of ubiquitin, and degradation by proteosomes.

1.12.1. Ubiquitination

Ubiquitin has a glycine amino acid on its carboxyl end, which forms an isopeptide bond between ubiquitin and the lysine residue on dysfunctional or misfolded protein via ATP hydrolysis. As seen in Figure 1.6. three enzymes are used in ubiquitination. First, the ubiquitin-activating enzyme (E1) collects inactive ubiquitin and activates it through the hydrolysis of ATP. Second, the ubiquitin-conjugating enzyme (E2) transfers the activated ubiquitin from E1. Third, ubiquitin-protein ligase (E3) shuttles ubiquitin onto the target protein. A stack of at least four ubiquitin proteins is needed for marking the target protein

for degradation, all of which are attached in the same manner. Ubiquitin stacks can also be attached to several lysine residues on the same protein [73].

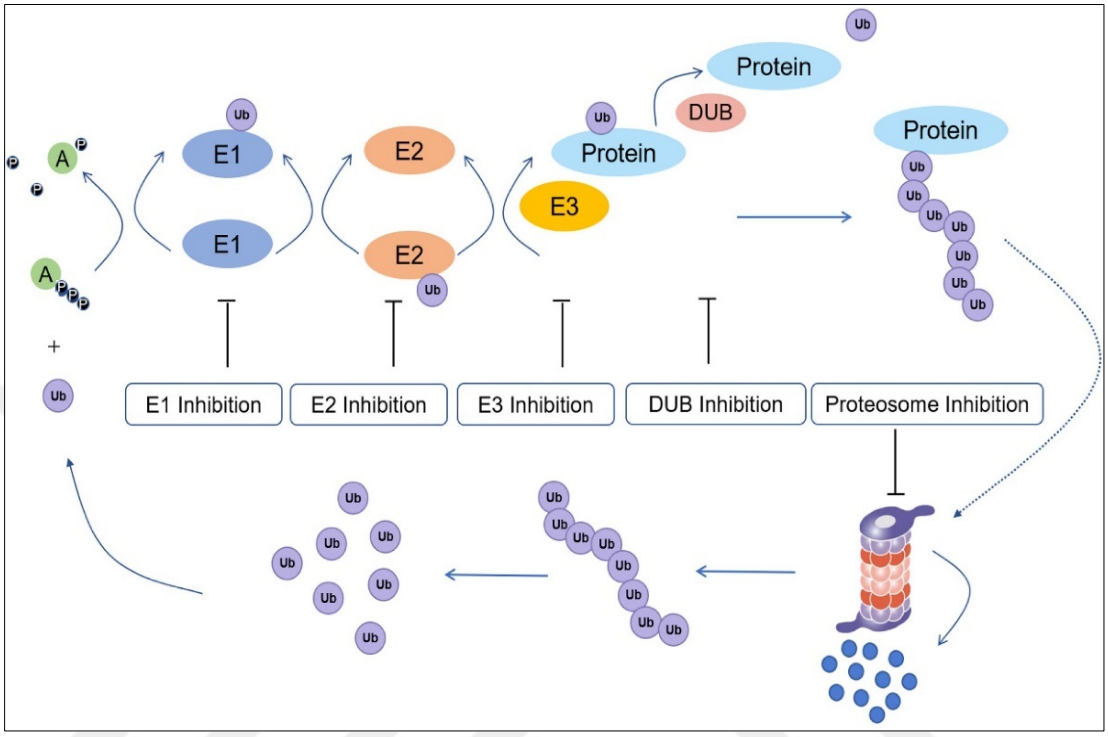

Figure 1.6. Ubiquitination process [64]

1.12.2. Ubiquitin Recognition

The 26S proteosome (made of a 20S barrel catalytic subunit sandwiched between two 19S regulatory subunits) is the protein complex responsible for ubiquitin recognition. This protein complex binds to its substrate (ubiquitin) via the 19S subunits, which unfold the target protein and linearize it to then pass it to the 20S barrel subunit, where degradation occurs [74].

1.12.3. Protein Degradation

Figure 1.7. illustrates that, in the 20S subunit, the target protein is cleaved into short 7-9 amino acid peptides and removes ubiquitin to be later recycled. The shredded protein is then released into the cellular matrix, and cellular proteases digest the peptides into their constituent amino acids, which can then be reused [75].

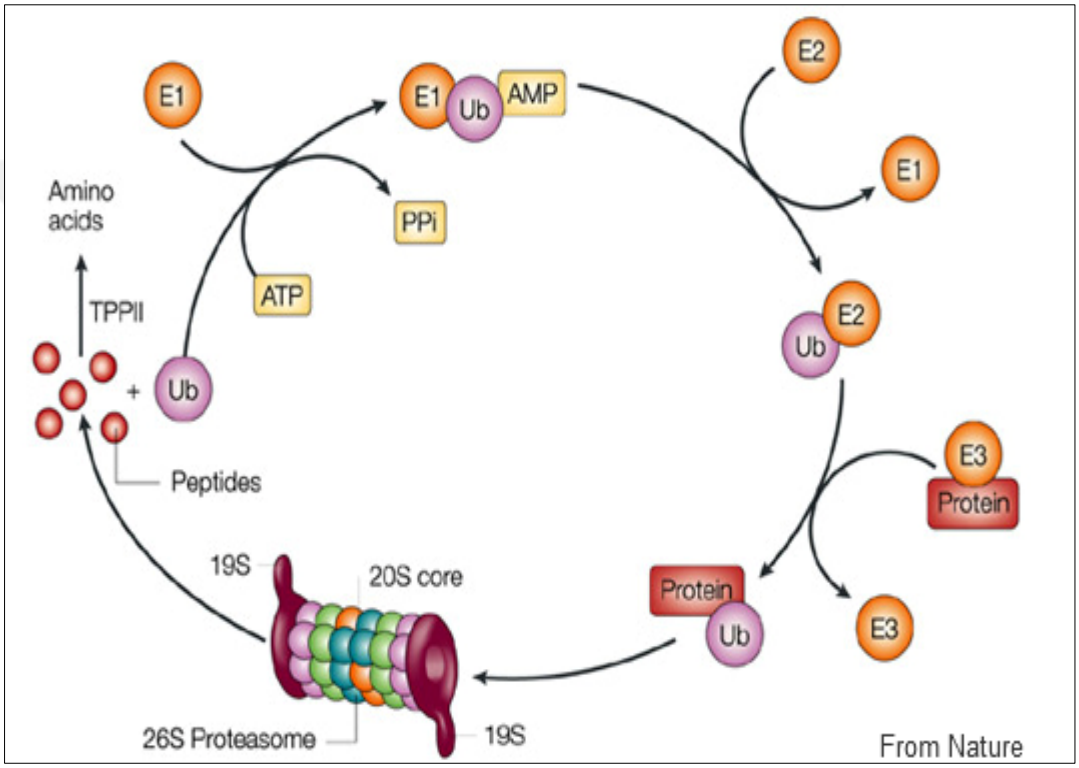

Figure 1.7. Full UPP Pathway [66]

1.13. PREVENTION OF HUMAN BABESIOSIS

Prevention of Babesiosis occurs in individual, residential, and civic tactics. Personally, isolation from tick-infested areas or areas populated by mice and deer, especially during the summer and spring from May to October. Immunocompromised or asplenic people must not travel to endemic regions. Wearing clothes covering the lower part of the body prevents ticks from latching onto the skin. Permethrin can be sprayed on the skin to defer ticks as well. Searching the body for ticks and removing them as soon as they latch also prevents infection.

Residentially, mowing the grass and fencing the house in deer-populated areas can reduce the risk of Babesiosis, and so does spraying acaricides to kill rodents in the house. Community-wise, expelling the local deer population has been shown to reduce the risk of Babesiosis since deer ticks are the primary host for B. microti [76]. People previously infected with Babesiosis are not allowed to donate blood as a transmission prevention precaution [58].

2. AIM OF THE PROJECT

The aim of the project is, bm-OTU like protein extraction, purification, and characterization which may lead to introduce some new approaches in treating the babesiosis disease in the future.

3. MATERIALS AND METHODS

3.1. PLASMIDS USED IN THE RESEARCH

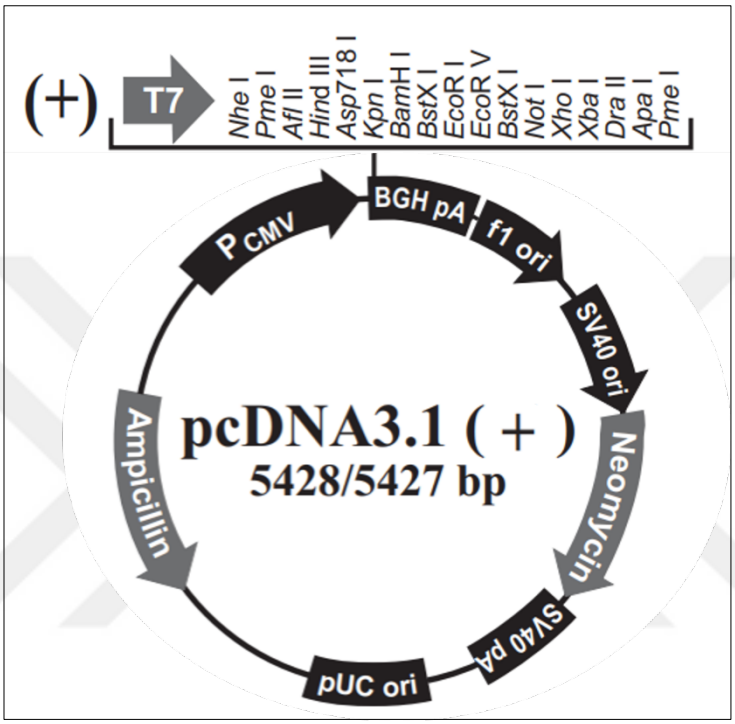

Figure 3.1. pcDNA vector map [58]

3.2. CLONING OF BM-OTU INTO A BACTERIAL VECTOR

Table 3.1. Analysis of the studied bm-OTU recombinant protein

Species	*Babesia microti*
Accession Number	CCF72503.1
Protein Description	unnamed protein product
Aminoacids	192 aa
Molecular Mass	22.06
Theoretical pI (ExPASy pI)	7.67

GPI anchor (GPI Lipid Anchor Project)	None
Predicted disulfide bonds (DiANNA 1.1)	68 - 153; 112 - 145 (Number of Cysteine: 5)

3.3. EXPRESSION OF THE RECOMBINANT PROTEIN

E.coli BL21 (DE3) and OrigamiTM (DE3) strains of competent cells were used to express the recombinant protein bm-OTU. In 5ml of LB broth, a smear of bacterial glycerol stock containing the bmOTU-pTE26b(+) was added with 5 µl of Kanamycin. Then they were incubated at 37˚C, 180 rpm, overnight. After incubation, the growth culture sample was transferred into a 1 L Erlenmeyer flask containing 1000 ml LB broth and 1000 µl Kanamycin. The sample was incubated in a shaker at 37˚C, and the optical density value was measured in different periods until the OD600 was equal to 0.6. Then 1mM IPTG was added to induce the expression level of the recombinant protein. The next day, the sample was placed in centrifuge tubes and centrifuged for 10 minutes at 6000 rpm at 15˚C. The supernatant was thrown after each centrifugation until all the solutions were finished. The pellets were resuspended with lysis buffer (8 M Urea, 20 mM Tris-HCL pH: 8.0), and sonication was performed for 7 minutes in the machine. In the final step, samples were centrifuged for 30 minutes at 13000 rpm at 6˚C, and the supernatant was kept in new tubes

for the purification procedure. Before and after IPTG induction, samples were collected for the next step.

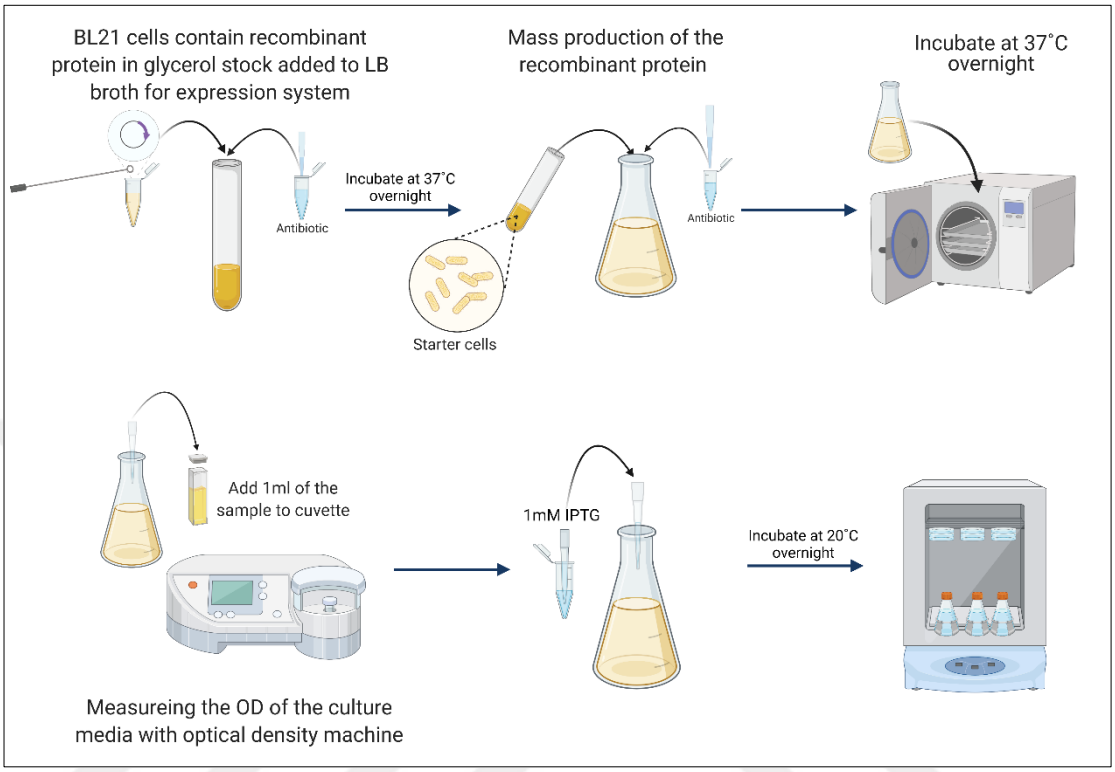

Figure 3.2. The workflow of recombinant protein expression into bacterial cells

3.3.1. SDS Gel Electrophoresis

After and before IPTG induction, samples were collected for performing SDS-PAGE. Samples were spun down, and the pellets were resuspended in 20 µl of 4x loading buffer. They were boiled for ten minutes and then spun at maximum speed for ten minutes. 12 percent SDS gel was prepared to separate the proteins by adding 10-25 µl per lane of the samples into each well of the polyacrylamide gel. The program was run at 100 volts for 120 minutes. After that, the gel was released from the apparatus and stained with Coomassie Brilliant Blue (CBB) solution at room temperature overnight. Then, CBB was removed, the gel was cleaned with distilled water once, and then the destaining buffer was added and left for 2 hours at room temperature to observe the results finally.

3.3.2. Western Blotting Analysis

Western blot was performed to validate the expression of the recombinant protein. Anti-HisTag antibody was used as the primary antibody for western blot analysis. After completing SDS-PAGE as mentioned before but without staining with Coomassie Brilliant Blue. A PVDF membrane was chosen since it is better for low molecular weight proteins and activated with methanol for 1 minute, followed by a 1X transfer buffer. The gel was directly placed on a PVDF membrane, and wet filter papers and sponges were used to assemble the transfer sandwich. The program was run for one hour at 100 volts, 400mA in an iced tank. After electrophoresis was completed, the transfer stack was disassembled, and the membrane was rinsed in 1X TBST and incubated for 1 hour in blocking buffer (5 percent milk solution) at room temperature. The membrane was incubated with primary antibody solution (1:1000 dilution in blocking buffer) at 4˚C overnight with gentle rocking. The PVDF membrane was washed with 1X TBST five times each for 5 minutes with gentle rocking to eliminate the non-specific background. Then the PVDF membrane was incubated with the secondary antibody solution (HRP) for one hour at room temperature with gentle rocking. Finally, the membrane was washed five times in 1X TBST buffer for 5 minutes. After incubating the membrane in the substrate as the manufacturer's directions, the chemiluminescence imaging system (ChemiDoc system) exposed the membrane and detected desired proteins.

3.4. ISOLATION AND PURIFICATION OF THE RECOMBINANT BM-OTU PROTEIN

The protein expression and extraction for bmOTU-pET26b(+) were performed according to the optimized conditions [58]. In brief, *E.Coli* BL21 cells with recombinant protein were grown at 37˚C overnight. IPTG induction was done at 20˚C overnight to obtain a large scale of protein expression. Harvested cells were exploded with lysis buffer (8 M Urea, 20 mM Tris-HCL pH: 8.0) and disrupted by sonication for 7 minutes in the machine. Samples were centrifuged for 10 minutes at 6000 rpm at 15˚C.

For purification of 6X His-tagged recombinant protein, the supernatant was filtered with 0.44µm syringe filters and then passed through a 5ml Ni-NTA agarose column (GE

Healthcare), washed two times with washing buffer (8 M Urea, 20 mM Tris-HCL pH: 8.0). Purifying the proteins was performed manually with binding buffer (8 M Urea, 500 mM NaCl, 50 mM Phosphate Buffer, 20 mM Imidazole, 14.1 uM 2-Mercaptoethanol) and elution buffer. After washing the Ni-NTA agarose column with washing buffer, the binding buffer was added to the top of the column, then the filtered supernatant was added to the column. The column was rewashed several times to add 1 ml elution buffer for four fractions.

Protein concentration was measured by the Bradford and bicinchoninic acid (BCA) assays using BSA as a standard solution. SDS-PAGE was performed for the collected fractions to check the purity of the proteins.

3.5. DESALTING AND ULTRA PURIFICATION

After purification, the collected fractions were desalted by substituting the elution buffer with PBS solution. Amicon Ultra columns (UFC501024 Amicon Ultra - 0.5 mL Centrifugal Filters) were used for desalting and ultra purification. 450µl of PBS buffer was mixed with 50µl of the purified protein in the column tubes. Then they were centrifuged for 25 minutes at 13000 rpm. The procedure was repeated three times, and finally, the column was moved upside down in a fresh tube and centrifuged. The desalted proteins were collected in PBS for proper folding.

3.6. FOLDING AND SOLUBILITY OF THE RECOMBINANT PROTEIN

Again PBS buffer was utilized to control the folding conditions of the desired proteins. basically, 25 µl of purified proteins were added to 475 µl of PBS in a 1.5 ml tube. The sample was incubated for one hour at 4˚C. Then, it was centrifuged at 14,000 rpm (maximum speed) for five minutes. The recombinant target protein is expected to be in the supernatant. 475 µl of the supernatant was carried out to a new Eppendorf, double distilled water was assorted with the precipitate, and SDS-PAGE protocol was accomplished.

3.7. CONCENTRATION MEASUREMENTS OF THE RECOMBINANT PROTEIN BY BCA ASSAY AND NANODROP

In order to find out the concentrations of the purified proteins, a BCA assay was performed. Firstly, BSA standard stock was prepared by taking a tiny amount (head of the spoon) of the BSA powder. The weight of the BSA powder was measured and diluted with PBS as follows; for each 2mg, 1 ml of PBS should be added. Serial dilution of the prepared BSA stock was done in 96 wells plate. The working solution was designed based on the 1:100 ratio of the A and B solutions. In the end, 5 µl of protein sample was added to 100 µl of working solution. The six-well plate was incubated at 37˚C for 30 minutes with gentle shaking. Measurements were carried out at 562 nm wavelength by spectrophotometer machine.

3.8. DUB-DETECTOR DEUBIQUITINASE ASSAY

Quantification of the enzymatic activity of the bmOTU protein was done by treating the

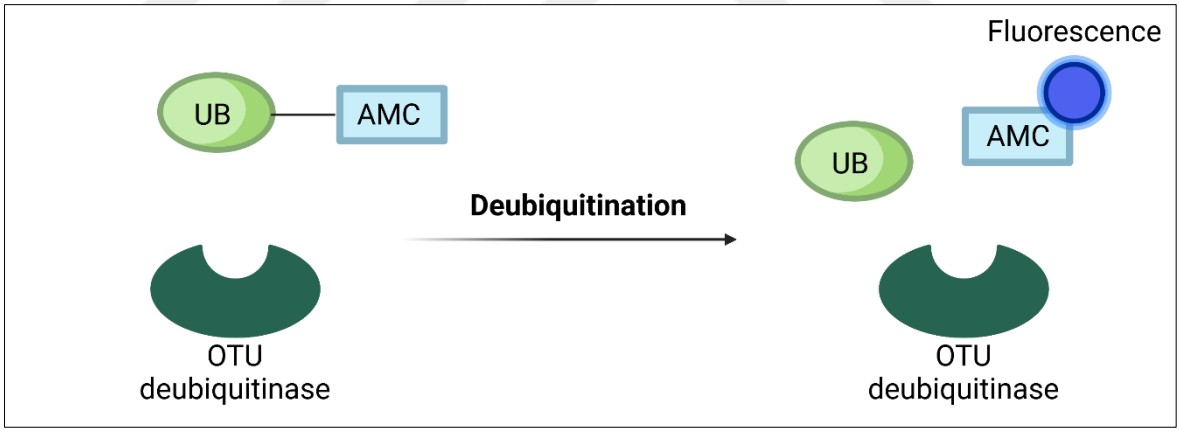

Figure 3.3. In vitro fluorescence deconjugation assay principle

purified protein with Ubiquitin-AMC substrate to detect the fluorescence by spectrophotometer machine.

The reaction sample consisted of a reaction buffer (10mM HEPES, 100mM NaCl, and 2.5mM DTT), a constant volume of protein sample, and a gradual volume of UB-AMC substrate in a final volume of 50 µl in 96 wells plate. By using Thermo™ Scientific™ Varioskan LUX, measurements were taken at 345nm excitation and 445 nm emission.

3.9. SUB-CLONING OF THE BM-OTU INTO MAMMALIAN VECTOR

bmOTU gene was transferred from bacterial expression vector to pcDNA3.1(+) mammalian expression vector via subcloning with restriction enzymes.

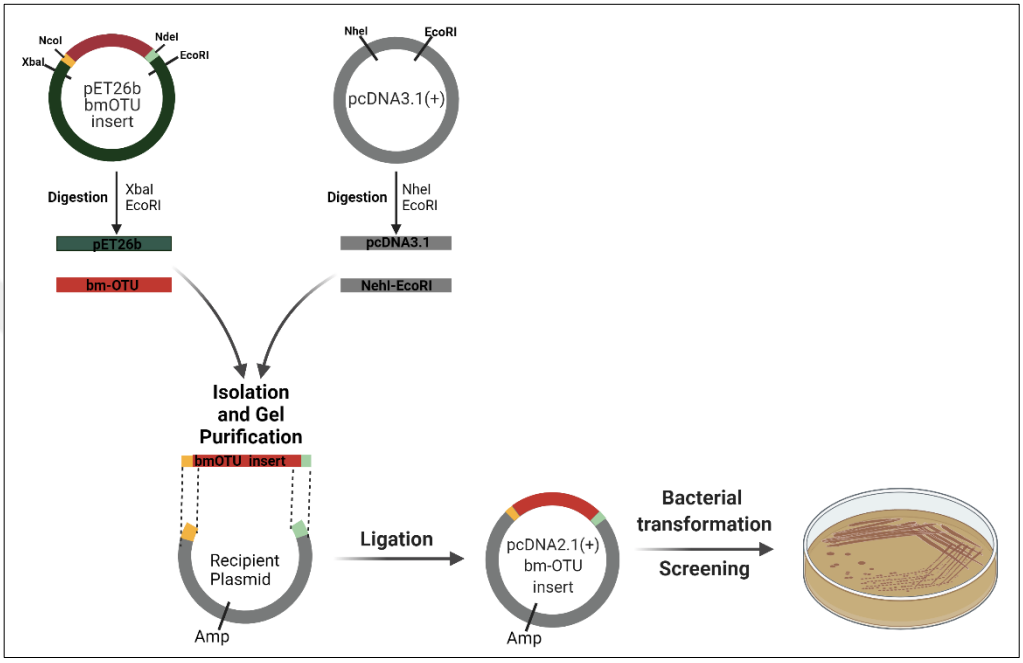

Figure 3.4. Sub-cloning of recombinant protein into pcDNA3.1(+) vector

3.9.1. Digestion with Restriction Enzymes

bm-OTUpET26b(+) vector was digested with XbaI (NheI compatible) and EcoRI overnight at room temperature with 30 µl of total reaction. Also, the pcDNA3.1(+) vector was digested with NheI (XbaI compatible) EcoRI overnight at room temperature. The amount of the donor plasmid was preferred to be 2-5 µg in order to cut it with both restriction enzymes. Gel electrophoresis was performed after incubation with 1 percent agarose gel.

3.9.2. Isolation and Gel Purification

All the digestion reaction was loaded in the agarose gel to increase the insert DNA and recipient plasmid yield. Gel purification was conducted by using Plasmid Gel Purification

Kit. The concentration of purified samples was measured, and they were placed at 4˚C for further steps.

3.9.3. DNA Ligation

DNA ligation was conducted to fuse the insert DNA to the recipient's plasmid backbone with a 3:1 (insert: plasmid backbone) ratio and 1.5-2 µg of total DNA in the reaction. The reaction contained vector DNA, insert DNA, 10X ligase buffer, T4 DNA ligase, and water-free. It was incubated at room temperature for four hours.

3.9.4. Transformation of the Recombinant Plasmid

Competent *E.coli* DH5α cells were used for transformation. 50µl of competent cells were mixed with 4 µl of DNA into the Eppendorf tube. The tube was placed on ice for 20-25 minutes and then on a heater for the heat shock process at 42˚C for precisely 60 seconds. 950 µl of LB broth was added to bmOTU-pcDNA3.1 plasmid mix and incubated in a shaker for 40-60 minutes at 37˚C. The media was centrifuged at 7000 rpm for one minute, the supernatant was discarded, and the pellet was resuspended very well. Then 100-200 µl was placed on an ampicillin agar plate and incubated at 37˚C overnight. Colonies were collected to obtain the desired plasmid.

3.10. TRANSFECTION OF THE RECOMBINANT PROTEIN INTO MAMMALIAN CELLS

3.10.1. Cell Thawing and Passaging

complete DMEM media was prepared by adding 10 percent FBS and 1 percent antibiotics into DMEM media. Then it was warmed to 37℃. HEK293T (+) cells were thawed at room temperature. Cells were removed into 5mL of complete prepared media and centrifuged at 1000 rpm for 5 minutes. The pellet was resuspended with 10mL of complete media, transferred in a 25T flask, and incubated in 37˚C, 5 percent CO2, and 95 percent RH incubator.

In order to maintain the cells healthy, it is essential to conduct passaging whenever the confluency approaches 80 percent. The Trypsinization method was used for passaging the HEK293T (+) cells. Media was removed from the flask, and 2 mL of trypsin was added with incubating for 5 minutes at 37˚C. 4 mL of complete media was added and spun down at 1500 rpm for 5 minutes.

3.10.2. PEI Transfection into HEK293T(+)

30 x 10^3 HEK293T(+) cells were seeded in a six-well plate with 2mL high glucose DMEM supplemented by 10 percent FBS (no antibiotics were added) and incubated at 37˚C overnight. In an Eppendorf tube, a 1:2 ratio (1mg/ml) of DNA: PEI was added to 200 µl of serum-free DMEM and incubated at room temperature for 15 minutes. The mixture was added dropwise to the culture media and incubated for 24 hours, and then the media was refreshed and incubated for an additional 72 hours. The cells were harvested by the trypsinization method for downstream applications.

3.11. APOPTOSIS ASSAY FOR FLOW CYTOMETER

After PEI transfection, the pcDNA-bmOTU plasmid was inserted into HEK293T(+). Cells from each well were collected and transferred to Eppendorf and then centrifuged at 1500 rpm for five minutes. Pellets were resuspended with 400 µl of 1X binding buffer and

centrifuged. Again pellets were resuspended with 50 µl of 1X binding buffer. 1 µl of Annexin V was added and waited for ten minutes in the dark, and then 2 µl of PI was added and stayed for three minutes only, and as in Table 3.2. results was observed by a flow-cytometer.

Table 3.2. Optimization of apoptosis stains for the pcDNA as control and pcDNA-bmOTU

	Annexin V	PI
pcDNA (control)	-	-
pcDNA (control)	+	-
pcDNA (control)	-	+
pcDNA (control)	+	+
pcDNA-bmOTU	+	+

3.12. WESTERN BLOT ANALYSIS FOR INVESTIGATING THE GENE EXPRESSION

Western blot was performed to identify intracellular deubiquitinase activity of the recombinant protein from the lysate cells that contained pcDNA and pcDNA-bmOTU plasmids. The transfected HEK293T (+) was harvested for western blotting.

3.12.1. Sample Preparation

The transfected HEK293T (+) was harvested for western blotting, washed with sterile PBS, and centrifuged for five minutes at 1500 rpm speed. The cell pellet was treated with RIPA buffer for 30 minutes on ice and then centrifuged the cell lysate mixture to collect the supernatant.

3.12.2. SDS-PAGE

SDS-PAGE was conducted to separate the proteins based on their molecular weight. 12 percent of polyacrylamide gel was used for loading the samples. 25 µg of proteins were mixed with 4X loading buffer and denatured by boiling them for five minutes at 95˚C. 20 µl of Samples were loaded per lane into each well of the polyacrylamide gel. The program was run at 100 volts for 120 minutes.

3.12.3. Transfer of Protein to the Membrane

After the SDS-PAGE was completed, proteins were transferred from the polyacrylamide gel onto the PVDF membrane. Membrane, filter papers, and sponges were saturated in 1X transfer buffer for 5-10 minutes during assembly of the transfer sandwich to perform the wet transfer. The program was run for one hour and a half at 100 volts, 400 mA in an iced tank.

3.12.4. Membrane Blocking

After electrophoresis was completed, the transfer stack was disassembled. The membrane was incubated for 1 hour in blocking buffer (5 percent milk solution) at room temperature, thus reducing or eliminating any non-specific proteins.

3.12.5. Primary and Secondary Antibody Staining

Poly-ubiquitinylated conjugates mAb (BML-PW8805-0500) and mono- and poly ubiquitinylated conjugates mAb (BML-PW8810-0500) were used as primary antibodies. Primary antibody solution (1:1000 dilution in blocking buffer) was added to the PVDF membrane and incubated at 4˚C overnight with gentle rocking. The PVDF membrane was washed with 1X TBST five times each for 5 minutes with gentle rocking to eliminate the non-specific background. Then the PVDF membrane was incubated with the secondary antibody solution (Anti-mouse IgG, HRP-linked antibody) at room temperature for 60 minutes with gentle rocking. Finally, the membrane was washed several times in 1X TBST buffer. After incubating the membrane in the substrate as the manufacturer's directions, the

chemiluminescence imaging system (ChemiDoc system) exposed the membrane and detected desired proteins.

3.13. REAL-TIME PCR FOR INVESTIGATING THE GENE EXPRESSION AT THE RNA LEVEL.

3.13.1. RNA Isolation

The transfected cells with recombinant protein were harvested for RNA isolation with trypsin and centrifuged for five minutes at 1500 rpm speed. The cell pellet was used to extract mRNA by using an RNA isolation kit (REF 740406.05).

3.13.2. cDNA Synthesis

ProtoScript II Frist Strand cDNA Synthesis Kit (Biolabs, Cat No: E6560) was used for reverse transcription with the aim of obtaining cDNA for further reactions.

3.13.3. Real-Time PCR Reaction

Selected genes were considered in order to design primers. Primers were defined from the NIH human primary storage database (http://humanprimerdepot.nci.nih.gov). The selected primers, as in Table 4.2, were requested from Sentegenbio and used for amplification of the cDNA product. The real-time PCR mixture included forward and reverse primers, PowerUp™ SYBR™ Green Master Mix (2X), cDNA product, and nuclease-free water. The real-time PCR reaction was performed as follows in Table 3.3.

Table 3.3. RT-PCR reaction

Program	Cycle	step
Preincubation	1	95 ˚C for 30s

Two steps Amplification	55	95 ˚C for 15s, 60 ˚C for 60s
Melting	1	95 ˚C for 10s, 65 ˚C for 60s, 97 ˚C for 1s
Cooling	1	37 ˚C for 30s

Lightcycle 96 Roche® detection device was used to perform the real-time PCR reaction. The Beta-actin gene was managed to be a control gene in qPCR analysis.

Table 3.4. List of selected primers

Gene	Forward Primer (5' – 3')	Reverse Primer (5' – 3')	Role in cellular immune response
AIM2	GCAGTGATGAAGACCATTCG	GGCTTTGGTTTTGTTACCGA	Cytosolic dsDNA sensor pathway
IL18	TGCAGTCTACACAGCTTCGG	ACTGGTTCAGCAGCCATCTT	Cytosolic dsDNA sensor pathway
NFKB1	ATGTATGTGAAGGCCCATCC	ATAACCTTTGCTGGTCCCAC	Antiviral response, cellular immune response pathway

IFNA1	CAGAGTCACCCATCTCAGCA	CTTGACTTGCAGCTGAGCAC	Type-I-Interferon signal pathway
IFNA2	GCTCACCCATTTCAACCAGT	CTTGACTTGCAGCTGAGCAC	Type-I-Interferon signal pathway
IFNAR1	GACCCTAGTGCTCGTCGC	ACTCATCGCTCCTGTTCCAC	Type-I-Interferon signal pathway
IFNB1	CTTTCGAAGCCTTTGCTCTG	CAGGAGAGCAATTTGGAGGA	Type-I-Interferon signal pathway
STAT1	TTCAGGAAGACCCAATCCAG	TGCTCTGAATATTCCCCGAC	Type-I-Interferon signal pathway
APOBEC3G	AGGGGCTTTCTATGCAACC	TTCCAAAAGGGAATCACGTC	Interferon-Stimulated Genes (ISG)
G1P2	GCGAACTCATCTTTGCCAGT	AGGGACACCTGGAATTCGTT	Interferon-Stimulated Genes (ISG)

IL15	AGAAGCCAACTGGGTGAATG	ACTTTGCAACTGGGGTGAAC	Interferon-Stimulated Genes (ISG)
BCL2L1	GAGCTGGTGGTTGACTTTCTC	TCCATCTCCGATTCAGTCCCT	Apoptotic genes
BCL2A1	TACAGGCTGGCTCAGGACTAT	CGCAACATTTTGTAGCACTCTG	Apoptotic genes
BAK	GTTTTCCGCAGCTACGTTTTT	GCAGAGGTAAGGTGACCATCTC	Apoptotic genes
BID	ATGGACCGTAGCATCCCTCC	GTAGGTGCGTAGGTTCTGGT	Apoptotic genes

4. RESULTS

4.1. EXPRESSION OF THE RECOMBINANT PROTEIN

E.coli BL21 (DE3) strain of competent cells was used extensively to express and produce the recombinant protein bm-OTU. Host cells with pEt26b-bmOTU plasmid were grown with Kanamycin up to 0.6 OD and induced with the appropriate quantity of 1 mM IPTG. After induction, the culture was incubated overnight at 24˚C; the pellet was suspended with a 4X loading buffer for protein expression profiles. Samples were resolved in 12 percent of acrylamide gel (Figure 4.1.). The expression of all proteins was analyzed on 12 percent SDS-PAGE, and the expression of recombinant protein band was observed as expected molecular weight compared to the protein marker. Many proteins have the same expression level in both non-induced and IPTG induction.

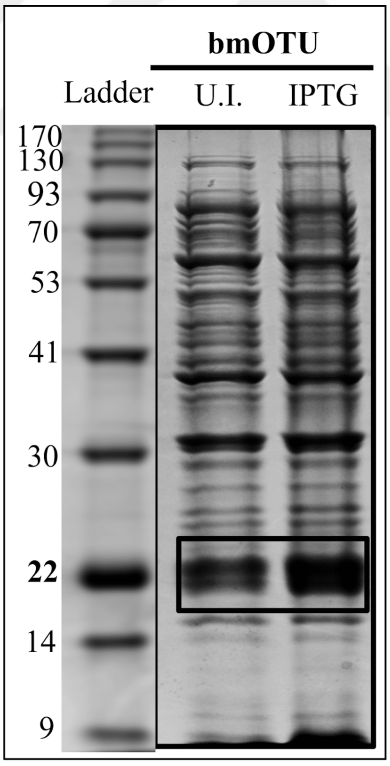

Figure 4.1. Analysis of the recombinant protein expression in BL21 bacterial cells before and after IPTG induction. The desired protein marked in the box. (U.I: Un-Induced, IPTG not added), (IPTG: Induced, IPTG is added)

Furthermore, the expression of the constructed recombinant protein with His-tag was validated in the western blotting result (Figure 4.2.)

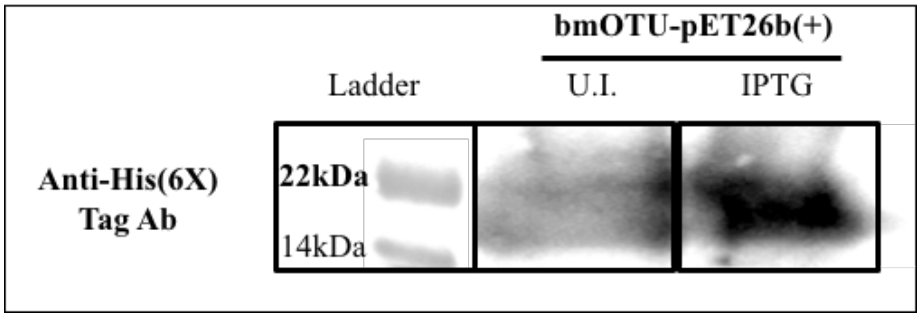

Figure 4.2. Western Blot analysis of bmOTU-pET26b(+). (U.I: Un-Induced, IPTG not added), (IPTG: Induced, IPTG is added)

4.2. ISOLATION AND PURIFICATION OF THE RECOMBINANT BM-OUT PROTEIN

Purification of the proteins was done manually by using the HisTrap HP Ni-NTA agarose column as described in section 3.3. Samples were collected after inducing the expression of the recombinant protein. Cell lysis was performed by sonic disruption for 7 minutes. Finally, the collected supernatant was filtered and used for purification through the Ni-NTA agarose column. With SDS-PAGE, elution fractions were shown in (Figure 4.3.), where F1 and F2 have a high concentration of bmOTU protein, and F3 and F4 have low concentrations. The result revealed significant 22 kDa bands of the purified recombinant protein. The purity of the elution fractions was sufficient compared to the lysate.

Ultra purification was performed through Amicon columns to increase the purity yield, which was observed in (Figure 4.3.) as there is only one bmOTU protein band. The result ensured the proteins were collected since the washing sample was regarded as an empty column in the gel. BSA (Bovine Serum Albumin) protein with 0.5 mg/ml was used to ascertain the concentration of the purified proteins, yet it was a bit much than 0.5 mg/ml.

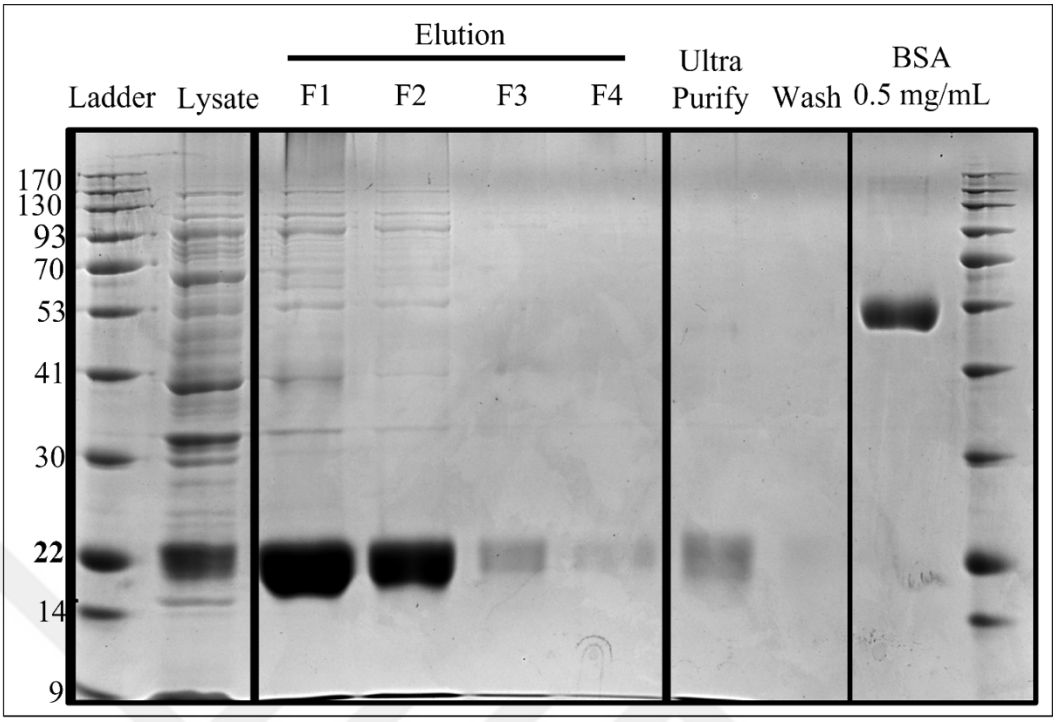

Figure 4.3. SDS-PAGE analysis of purification process for recombinant protein

4.3. CONCENTRATION MEASUREMENTS OF THE RECOMBINANT PROTEIN WITH BCA ASSAY

BCA assay was conducted to demonstrate the concentrations of the purified proteins by using BSA as a standard solution. The absorbance of the samples was measured by a spectrophotometer, and the standard curve was drawn with known concentrations of the BSA as in (Figure 4.4.). From the linear equation of the standard curve, the concentration of the recombinant OTU protein with HisTag was calculated and obtained as in (Table 4.1.).

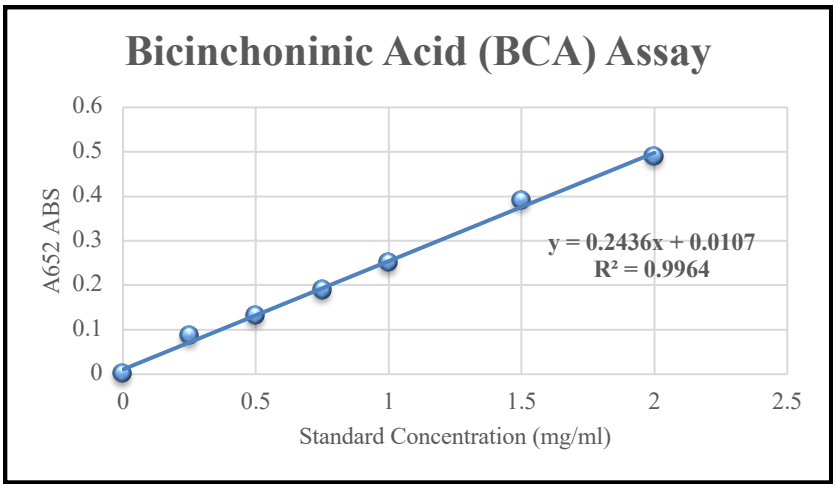

Figure 4.4. Standard curve of the BCA assay

Table 4.1. Measurements of the BCA assay of the purified protein

	Absorbance (nm)	**Concentration (mg/ml)**
Measurement 1	0.267	1.09
Measurement 2	0.323	1.33
	Average	**1.21**

4.4. INVESTIGATION OF FOLDING AND SOLUBILITY OF BM-OTU RECOMBINANT PROTEIN

In this experiment, the folding and solubilization were detected after removing the chaotropic salts and urea from the purified protein fractions using desalting columns (Amicon filters). Protein with proper folding results in a stable soluble protein, and thus the recombinant OTU protein was tested using PBS. 25 µl of purified proteins were mixed with 175 µl of PBS in a 1.5 ml tube. The sample was incubated for one hour at 4˚C. Then, it was centrifuged at 14,000 rpm (maximum speed) for five minutes.

The recombinant target protein was expected to be in the supernatant. 175 µl of the supernatant was carried out to a new Eppendorf, and distilled water was mixed with the precipitate. Analysis of SDS-PAGE exposed a fuzzy band that represents the bmOTU protein in the supernatant and a fair column in the pelleted part based on their molecular weight.

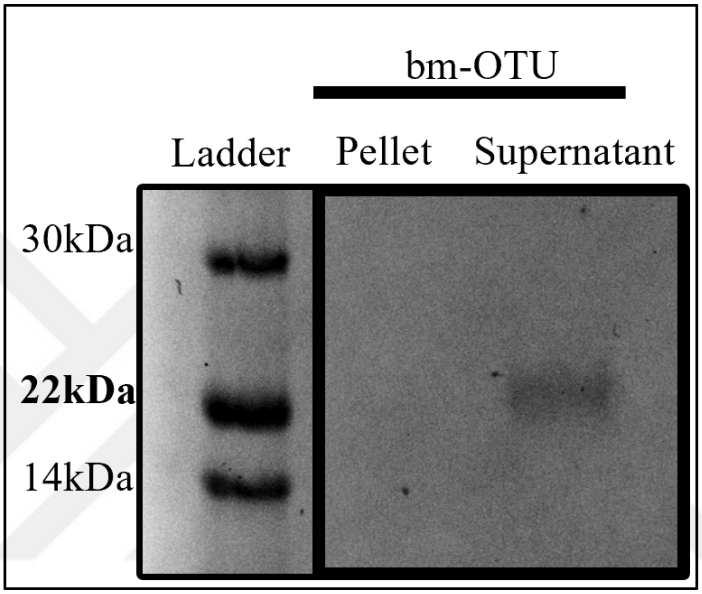

Figure 4.5. SDS-PAGE analysis for protein folding of the purified bm-OTU

The supernatant and pellet concentration was measured using nanodrop at protein A280. Then the values of the supernatant were divided by the pellet concentration in order to calculate the solubility factor. The formulation of the solubility factor " supernatant (mg/ml) * 100 / (supernatant + pellet(mg/ml))" was used for calculating the bmOTU concentrations (Figure 4.5.). As a result, the bmOTU protein sample was approximately 93 percent soluble in PBS (Figure 4.6.). The solubility factor percent was considered adequate for addressing the functionality of the bmOTU protein.

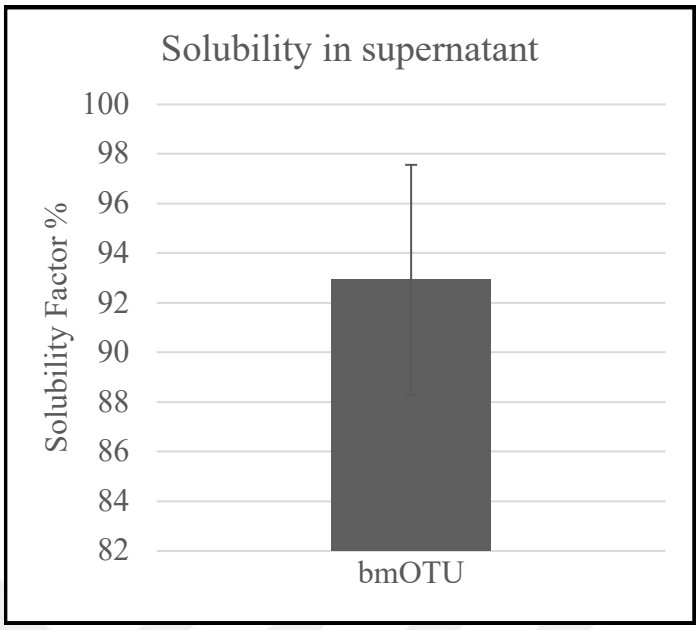

Figure 4.6. The solubility factor of purified recombinant OTU protein

4.5. DUB-DETECTOR DEUBIQUITINASE ASSAY

The deubiquitinase activity of Babesia microti OTU protein was quantified by measuring the fluorescence of Ubiquitin-AMC substrate. Fluorescence happened during the emission of light at 346 nm for excision and emission at 446 nm in a kinetic mode of the prepared sample. The process of disjoining the AMC from the UB-AMC substrate can exposure emission after excitation, and thus the bm-OTU protein is a deubiquitinating enzyme.

The reaction consisted of a constant volume of a reaction buffer, a constant protein sample, and a gradual volume of UB-AMC substrate (50 µM; 50 µg) in a final volume of 50 µl in 96 wells plate. Nothing was added in the well for a blank; only reaction buffer, Ub-AMC, and bm-OTU were used as controls for enzymatic analysis. The activity of bm-OTU was not observed any increase after 6 hours of measuring (Figure 4.7.); it started from a high point of RFU compared with the control measurements.

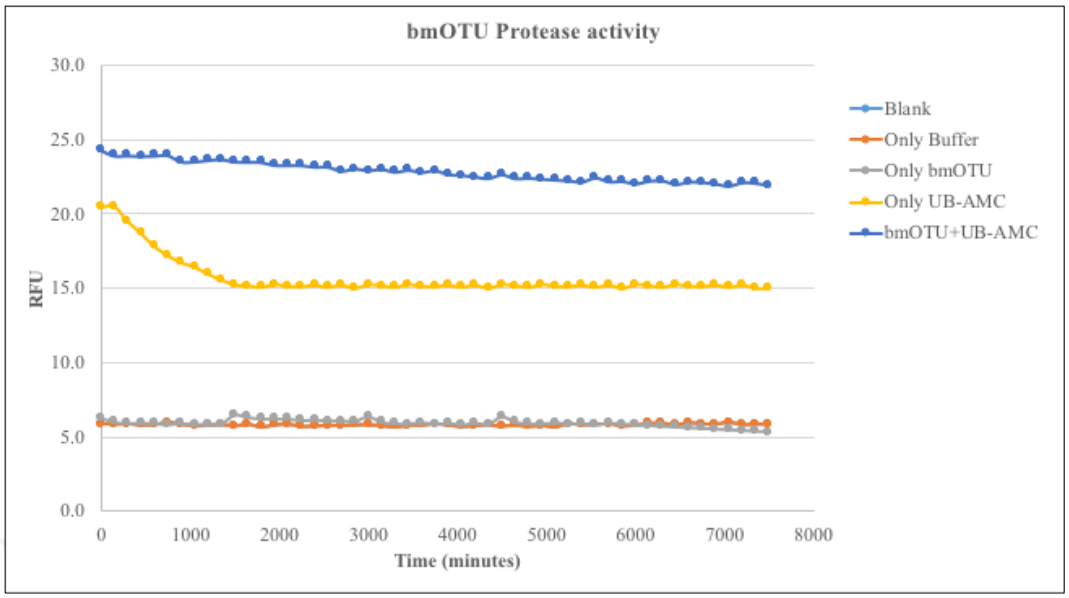

Figure 4.7. Analysis of deubiquitination activity of bm-OTU protein

The t-test was used for analyzing the obtained data, and the results showed (Figure 4.8.) p-value as $p < 0.005$ and standard deviation as 0.124. Thus the enzymatic activity of the recombinant bm-OTU protein was detected but not as high as expected in this project.

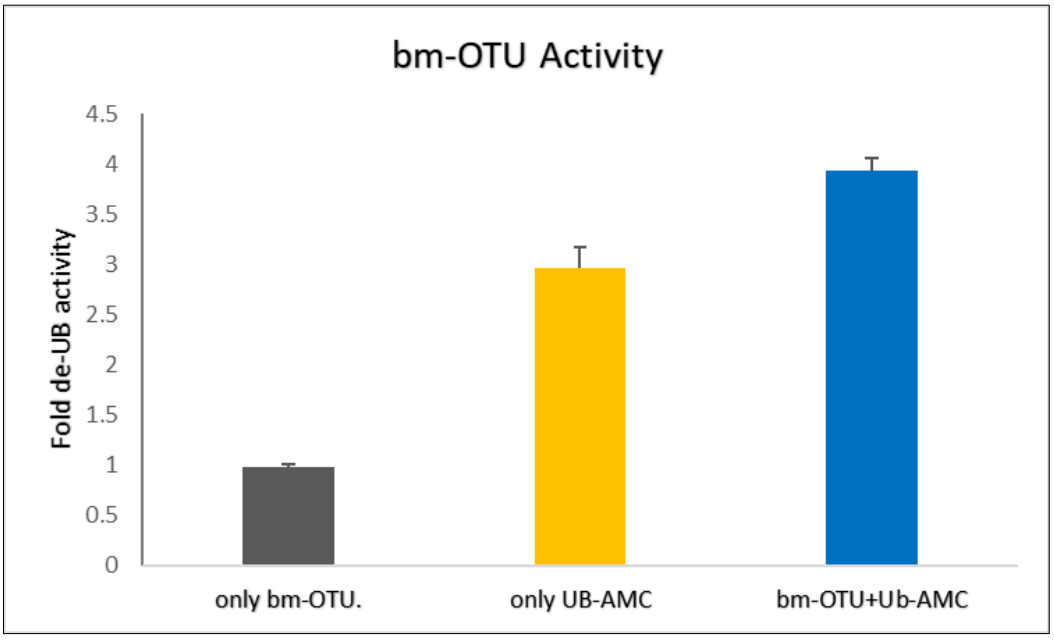

Figure 4.8. nalysis of the de-UB activity of bm-OTU protein compared to the control

4.6. CLONING OF THE BM-OTU INTO MAMMALIAN VECTOR

To test the OTU protein's activity and its ubiquitinylation properties, the bm-OTU protein was inserted into a mammalian expression vector (pcDNA3.1(+)) using subcloning. Briefly, the bm-OTU was excised from the pEt26b(+) vector by using XbaI and EcoRI restriction enzymes and obtained by gel purification of the loaded samples as in shown in (Figure 4.9.).

On the other hand, the pcDNA3.1(+) vector was digested with proper restriction enzymes, which are NheI and EcoRI, and these enzymes are shown in (Figure 4.9.) as a pcDNA3.1(+) vector map. Two different samples were loaded in gel electrophoresis to check the digestion event of the uncut and cut plasmids of bm-OTU pEt26b(+). In this way, the bm-OTU fragment was obtained for subcloning (Figure 4.10.). The uncut pcDNA3.1(+) vector and its double digestion were also observed in gel electrophoresis in high dense bands (Figure 4.11.).

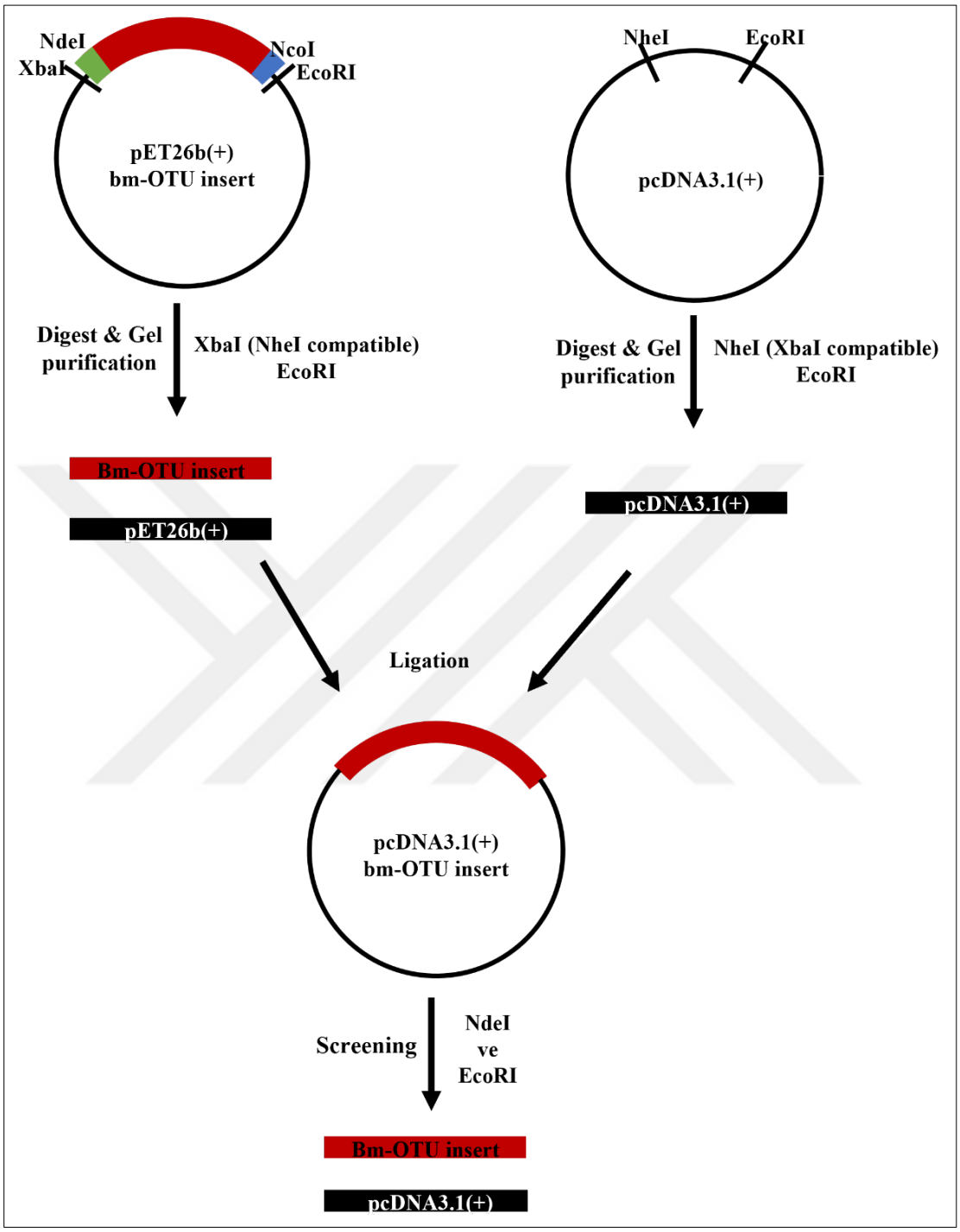

Figure 4.9. Cloning of the recombinant protein into mammalian vector

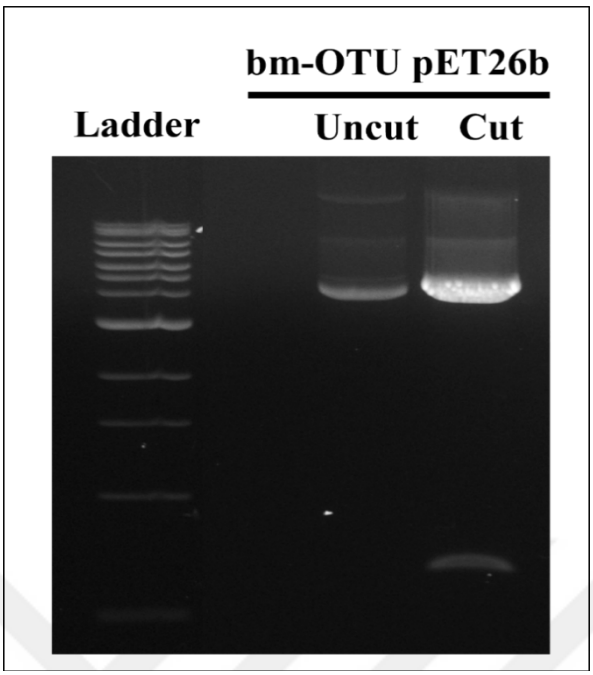

Figure 4.10. Analysis of bm-OTU pET26b in Agarose gel after using XbaI (NheI compatible) and EcoRI restriction enzymes. (Uncut: RE not added), (Cut: RE are added)

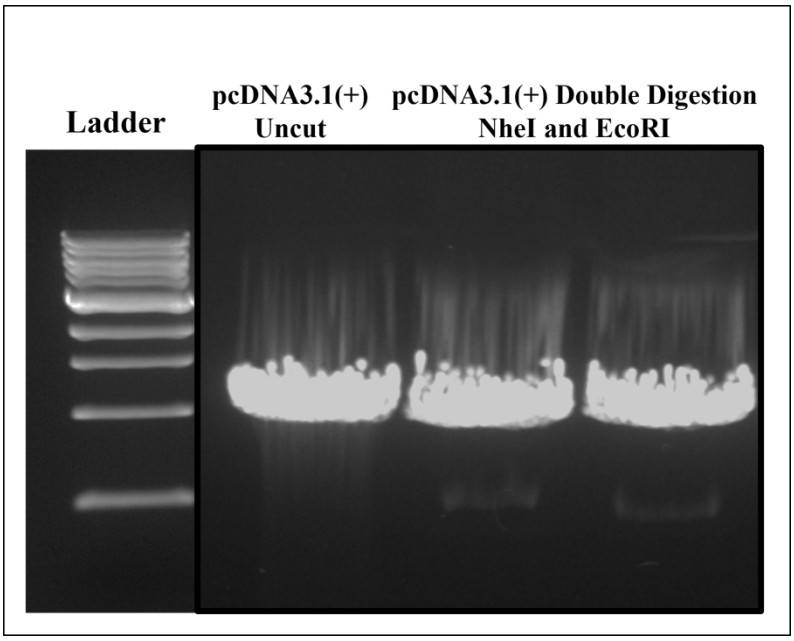

Figure 4.11. Digestion of the pcDNA3.1 (+) mammalian vector with NheI and EcoRI enzymes

As a final step of this subcloning, DNA ligation was conducted to fuse the insert DNA to the recipient's plasmid backbone with a 3:1 (insert: plasmid backbone) ratio and 1.5-2 µg of total DNA in the reaction. The reaction was contained vector DNA, insert DNA, 10X ligase buffer, T4 DNA ligase, and water-free. The incubation was at room temperature for four hours. Samples with double digestion and single digestion (EcoRI, NdeI) were loaded. The result was observed as in Figure 4.12. three bands for the double digestion, two bands for NdeI single digestion, and only one thick band for uncut pcDNA3.1(+) and EcoRI single digestion.

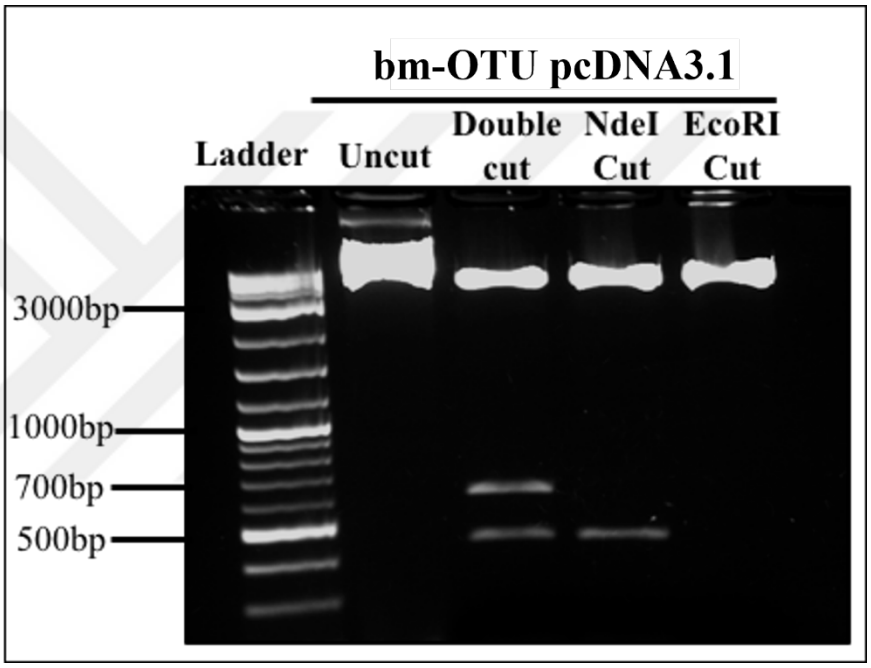

Figure 4.12. Agarose gel analysis of bm-OTU pcDNA3.1 with single and double digestions (with NdeI and EcoRI enzymes)

4.7. PEI TRANSFECTION INTO HEK293T CELLS

As mentioned above, inserting the recombinant protein of OTU into the pcDNA3.1(+) vector was performed to test several properties in mammalian cells. The constructed bm-OTU pcDNA3.1 plasmid was transfected into 30 x 10^3 seeded HEK293T human cells in a six-well plate with 2 mL high glucose DMEM supplemented by 10 percent FBS (no antibiotics were added) by using the PEI transfection technique. Green fluorescent protein was used to check the transfection efficiency with PEI ratio (1:2).

The results were obtained after 24 hours for transfected GFP and bm-OTU pcDNA3.1, and the efficiency was approximately 70 percent compared to the confluency of the cells (Figure 4.13.). Moreover, the media was refreshed and incubated for an additional 72 hours, and then cells were harvested by the trypsinization method for downstream applications.

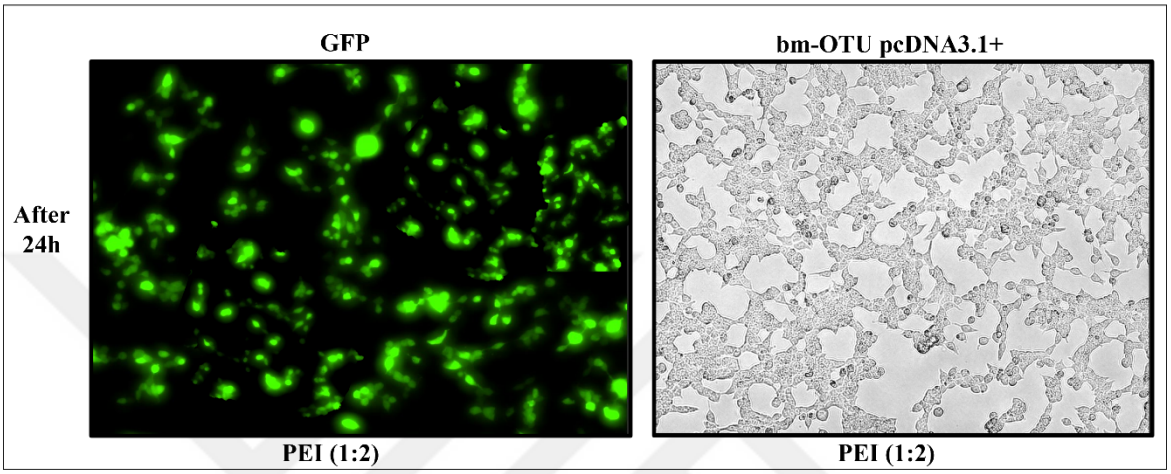

Figure 4.13. Transfection analysis under microscopy for GEP and bm-OUT pcDNA3.1 vectors into HEK293T mammalian cells

4.8. APOPTOSIS ASSAY FOR FLOW CYTOMETER

After transfection of the bm-OTU pcDNA3.1 into HEK293T human cells, the bm-OTU pcDNA3.1's effects were detected and quantified by using an apoptosis assay. pcDNA3.1 was used as a control to compare the changes in HEK293T cells. Approximately 70 percent

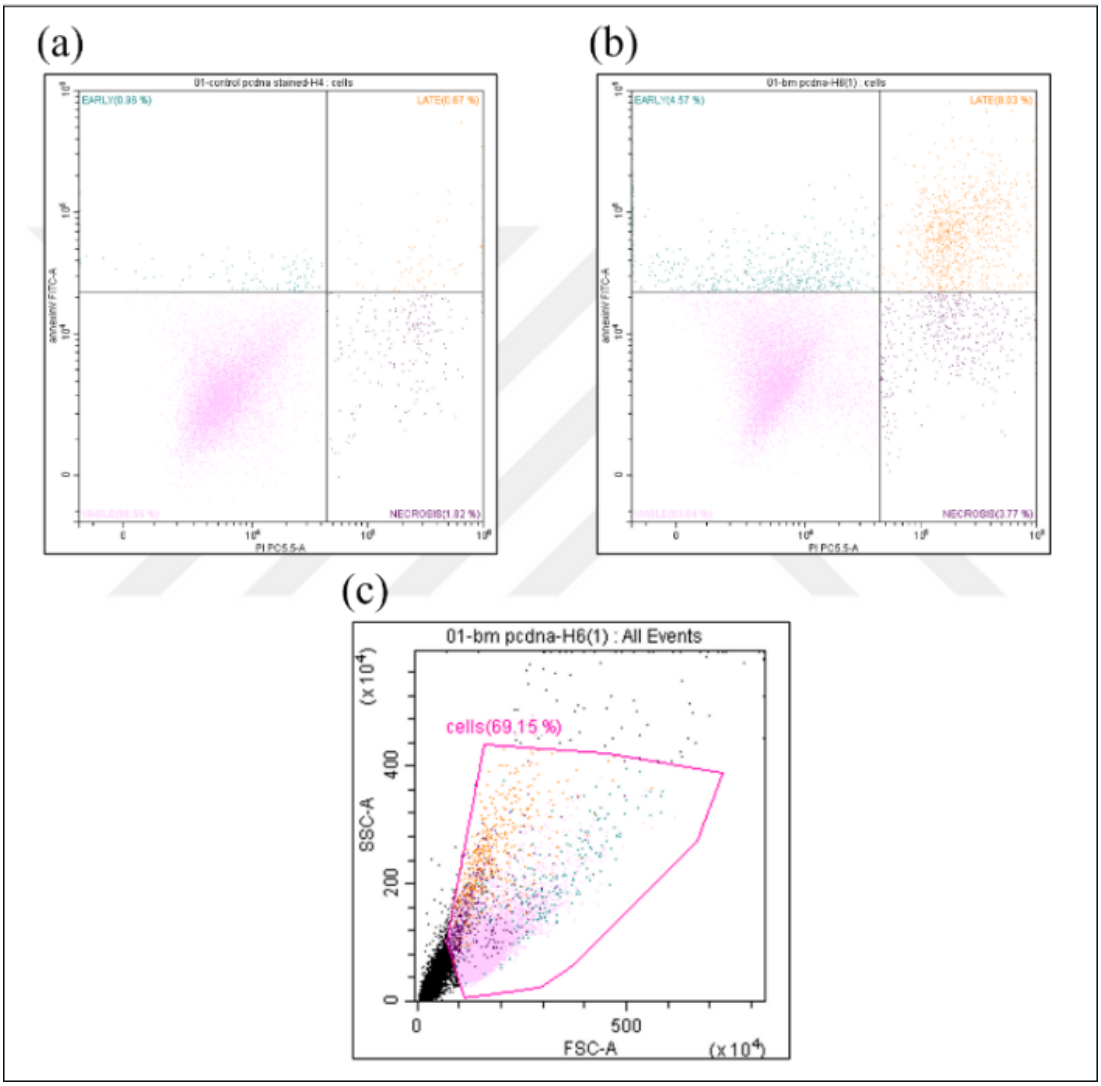

Figure 4.14. Quantification of the PEI transfection of bm-OTU pcDNA3.1 into HEK293T cell, (a) quantification of number of cells for the four stages as a control, (b) quantification of number of cells for the four stages of bm-otu pcDNA3.1, (c) total number of the h

of cells were selected for apoptosis measurements (Figure 4.14.). There is a significant effect

of the bm-OTU pcDNA3.1 vector on these cells on early, late, and necrosis apoptosis levels seen in (Figure 4.15.).

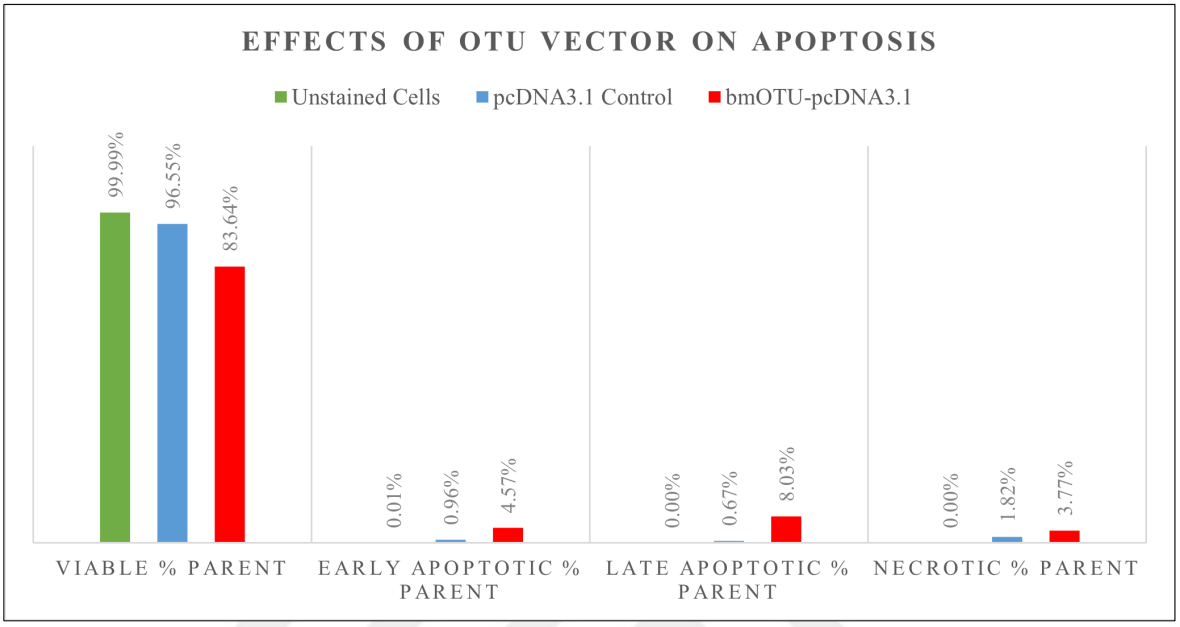

Figure 4.15. Effects of the transfected bm-OTU pcDNA3.1 on apoptosis in HEK293T mammalian cells in four different stages

4.9. WESTERN BLOT ANALYSIS FOR INVESTIGATING THE GENE EXPRESSION

The transfection procedure was repeated to perform a western blot using anti-ubiquitin Antibodies. After three days, the cell samples that contained the pcDNA3.1 vector used as a negative control and bm-OTU pcDNA3.1 were harvested for western blot analysis.

The anti-ubiquitin antibody was ordered from Enzo Life Sciences with serial number BML-PW8810-0500. The BML-PW8810-0500 was used as mono- and polyubiquitinylated conjugates monoclonal antibody (FK2); thus, Both mono and polyubiquitin proteins are recognized.

The intracellular deubiquitinase activity of the recombinant protein was determined using the BML-PW8810-0500 antibody. The antibody only binds to ubiquitin-bound protein and has no effect on ubiquitin in its free form.

Beta-Actin (42 kDa) was used as a loading control for both transfected cells (pcDNA3.1, bm-OTU pcDNA3.1) since it is found in all eukaryotic cell types and has a broad range of expression. Another reason why this protein is appropriate loading control is that the expression levels of this protein do not change much when cells are treated.

As shown in the results (figure 4.16.), the beta-actin protein was observed in all samples with bands size of 40-42. The anti-Ub (BML-PW8810-0500) antibody resulted in the pcDNA3.1 and bm-OTU pcDNA3.1 samples showing smear bands due to its recognition property. The BML-PW8810 antibody was used to identify the mono-poly ubiquitination,

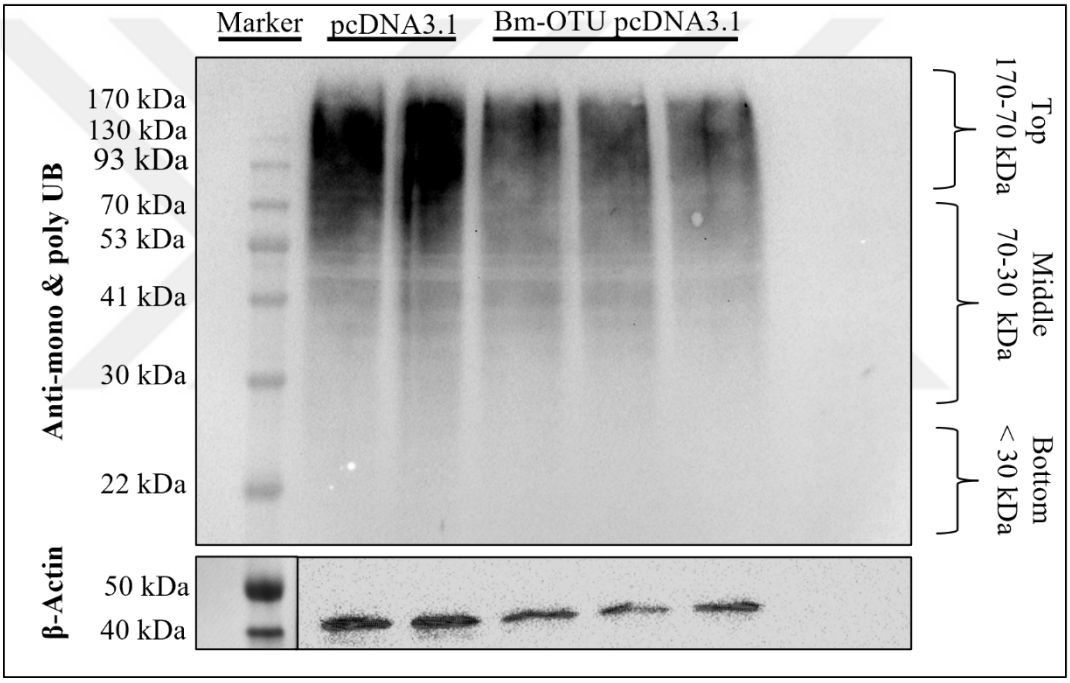

Figure 4.16. Effects of bm-OTU protein on intracellular ubiquitination by using mono-poly-Ub antibody, effects are divided into three parts in the western blot analysis, Beta actin is used as a control.

and the western blot result was divided into three regions based on the size and the density of the proteins (Figure 4.16.). The top region was selected for proteins greater than 70 kDa, the middle region was for all proteins with size of 70-30 kDa, and the bottom region bands were selected for proteins less than 30 kDa. In all regions, it was perceived to have fewer proteins of bm-otu pcDNA3.1 compared to the negative control.

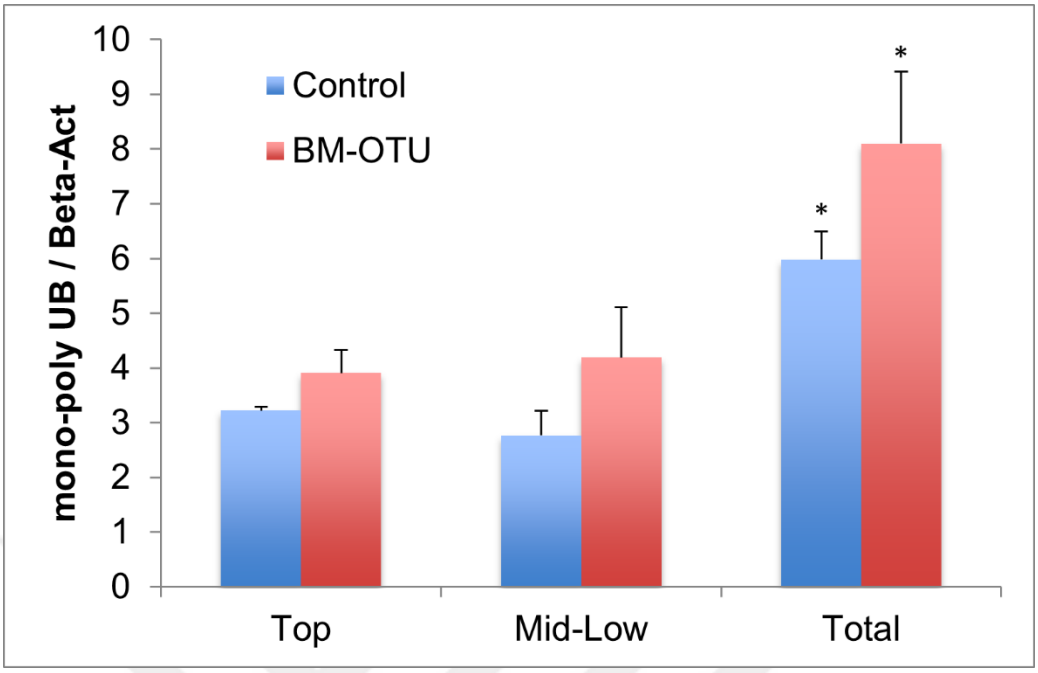

Figure 4.17. Quantitative analysis of the effects of bm-OTU protein on intracellular ubiquitination by using mono-poly-Ub antibody, top region for for proteins greater than 70 kDa, middle and bottom regions for proteins proteins less than 70 kDa. * $p < 0.05$

The amount of poly-UB and the band density was determined in detail in the three regions using the ImageJ program (Figure 4.17.).

4.10. REAL-TIME PCR FOR INVESTIGATING THE GENE EXPRESSION

Analysis of gene expression in HEK293 mammalian cells after transfection of pcDNA3.1 vectors with bmOTU sequence was performed to determine the effect of recombinant OTU protein on cell and molecular responses, recognize molecular mechanisms of action and exemplify de-UB activity.

After transfection, the results of RT-PCR for genes involved in the cellular immune pathway have seen considerable transcriptional alterations (Figure 4.18.). The result shows the AIM2 gene from the pyroptosis pathway has an increase compared to the control; in contrast, the IL18 also from the pyroptosis pathway genes has an increase in the bmOTU-pcDNA3.1.

There was no change in most cellular immune response genes; however, IFNAR1 and NFKB1 genes were slightly decreased in the expression level.

Additionally, there was an overall decrease in interferon stimulatory genes STAT1, and IL15, while the expression of APOBEC3G and C1P2 reduced considerably. Lastly, most apoptotic genes remained unchanged, like BCL2L1, BCL2A1, and BID, but the expression of the BAK gene was dramatically increased, which means an overexpression of the gene.

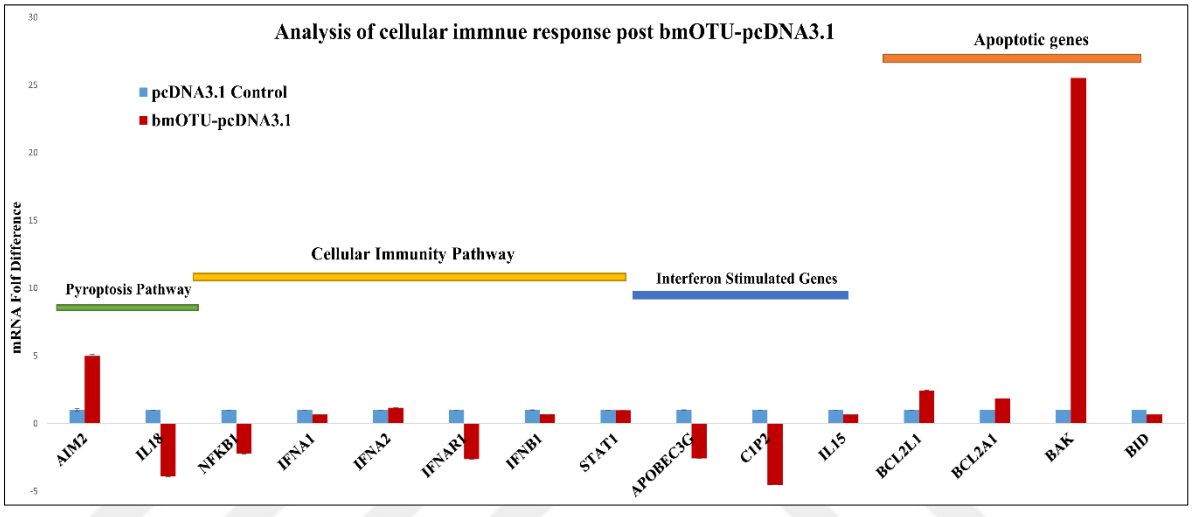

Figure 4.18. Effects of bm-OTU protein on the cellular immune pathways for different selected genes expression

5. DISCUSSION

The purpose of this study was to characterize the novel bm-OTU-like protein *in vitro* and *in vivo* and mainly its deubiquitination activity. The study represents the first direct demonstration of bm-OTU protease effects on the intracellular ubiquitination at the mono-poly-UB level and cellular immune pathways. Inhibition of this protease activity was planned in this study to develop new approaches for treating babesiosis disease. However, further improvement is expected to result in an improved understanding of the DUB activity because of a potential limitation. The study, therefore, highlights the importance of understanding the activity of bm-OTU-like protease.

The *Apicomplexan* pathogens that include *babesia microti* [77] are intercellular parasites, and they are comparable to Crimean Congo Haemorrhagic Fever Virus (CCHFV) [78]. Several Viral OTU-related proteins were reported and showed that these proteins have the ability to alter the ubiquitination process and cleave the region of the ISG15 in the infected cells and it was proved that CCHFV has OTU de-ubiquitination activity when cells are invaded. In addition, the OTU deubiquitinase Y89-W99 pockets were determined as a significant role in developing small molecules inhibitors for treating the diseases [58,63]. *Babesia Microti*, an unnamed protein product, was predicted to be from the OTU-like cysteine protease [80]. This is the first time that *babesia microti* OTU protein has been identified and characterized.

The results of the present study support the hypothesis that; if the CCHFV can use the deubiquitinase pocket to invade the cells, *babesia microti* (*B.microti*) OTU protein can also has the OTU de-ubiquitination activity since there are similarity between CCHFV and Viral OTU-like proteases as it shown in (Figure A.2). Also, an alignment was established for several viral OTU protein sequences and *babesia microti* OTU-like protein sequences. Interestingly, particular amino acids in the OTU deubiquitinated pockets that are used for inhibition of these proteins have similar domains among CCHFV OTU protein and *Apicomplexan* pathogens, specifically *B.microti.* The results are interesting and help justify the conservation of OTU-like proteins and CCHFV OTU proteins in which specific amino acids share common domains in the conserved sequences [61,63,81].

Initially, cloning the bm-OTU gene in the pET26b(+) vector was done successfully before starting this study. The obtained pET26b(+) bm-OTU recombinant protein was sequenced and checked for nucleotide errors. pET26b(+) vector was used in this experiment as an expression vector for sufficient recombinant protein production [82]. Subsequently, the constructed recombinant protein was transformed into BL21 *E.coli* strain of competent cells, and colonies were selected from LB kanamycin(+) plates for protein expression and mass production of the bm-OTU protein. Host cells with pEt26b-bmOTU plasmid were grown with Kanamycin up to 0.6 OD and induced with the appropriate quantity of 1 mM IPTG [61]. The result demonstrates the adequacy of the method for protein production using IPTG induction.

The expression of all proteins was analyzed on 12 precent SDS-PAGE, and the expression of recombinant protein band was observed as expected molecular weight compared to the protein marker as 22 kDa. Many proteins have the same expression level in both non-induced and IPTG induction which means they can not overexpressed with the IPTG. Also, the expression of the constructed recombinant protein with His-tag with IPTG induction was validated in the western blotting result.

A plethora of measures has been developed to assess the purification of the recombinant protein. Firstly, purification of the recombinant protein was done manually using the HisTrap HP Ni-NTA agarose column, several fractions were obtained in this stage where F1 and F2 have a high concentration of bmOTU protein, and F3 and F4 have low concentrations as expected since the protein are eluted at the beginning. The result revealed significant 22 kDa bands of the purified recombinant protein. The purity of the elution fractions was sufficient compared to the lysate, and thus protein purification was completed favorably. Secondly, Ultra purification was performed through Amicon columns to increase the purity yield of the recombinant protein. The result did yield the expected improvement in the protein purity, but the concentration of the protein was low approximately the half, compared to the previous samples. Also, the result ensured the proteins were collected since the washing sample was regarded as an empty column in the gel. BSA (Bovine Serum Albumin) protein with 0.5 mg/ml was used to ascertain the concentration of the purified proteins, yet it was a bit much than 0.5 mg/ml. Thirdly, BCA assay was conducted to demonstrate the concentrations of the purified proteins by using BSA as a standard solution. The standard curve was plotted with known concentrations of the BSA and the concentration of the

recombinant OTU protein with HisTag was calculated and obtained as an average of 1.21 mg/ml.

Finally, the protein solubility is substantial for maintaining the protein conformation in the field of structural biology. Functional proteins have folded and soluble features simultaneously. Any failure in the protein solubility or inactive formation of the protein frequently results in protein misfolding and indirect aggregation, and thus affect the overal kinetic acitivity [82–84]. Protein with proper folding results in a stable soluble protein, and thus the recombinant OTU protein was tested using PBS. The recombinant target protein was expected to be in the supernatant. Analysis of SDS-PAGE confirmed the protein solubility by exposing a fuzzy band that represents the bmOTU protein in the supernatant and a fair column in the pelleted part based on their molecular weight.

The deubiquitinase activity of Babesia microti OTU protein was quantified by measuring the fluorescence of the Ubiquitin-AMC substrate. The process of disjoining the AMC from the UB-AMC substrate can produce exposure emission after excitation, and thus the bm-OTU protein is a deubiquitinating enzyme. The test of the enzymatic activity for the recombinant bm-OTU protein was shown a slight activity compared with the result of only UB-AMC acitivty but the acitivty of the recombinant bm-OTU protein was not sufficient as expected in this project. Based on the data obtained, the method cannot be recommended for use in detecting the bm-OTU protease activity. In this manner, some improvements and changes could be made in the expression and production level to increase the solubility, and thus obtaining a proper folding. Also, concentration of the recombinant bm-OTU protein can be increased to get a better result. Temperature and period of the reaction can improve the DUB activity. Therefore, those changes during DUB assay could contribute in a positive result.

To test the OTU protein's activity and its ubiquitinylation properties, the bm-OTU protein was instered into a mammalian expression vector (pcDNA3.1(+)) using subcloning. As a final result of this subcloning, bm-OTU pcDNA3.1(+) plasmid was obtained efficiently. The constructed bm-OTU pcDNA3.1 plasmid was transfected into HEK293T human cells because of its high transfectability, immortalized cell line and fast growing [85]. The transfected system was based on using PEI reagent regardless of its toxicity but it has high transfection efficeincy in HEK293T human cell lines [86]. The result was obtained after 24 hours transfected GFP and bm-OTU pcDNA3.1, and the efficiency was approximately 65

precent compared to the confluency of the cells which means the transfection was done successfully. After transfection of the bm-OTU pcDNA3.1 into HEK293T human cells, the bm-OTU pcDNA3.1's apoptosis effects were detected and quantified in both visual and numerical results. pcDNA3.1 was used as a control to compare the changes in HEK293T cells. Approximately 70 percent of cells were selected for apoptosis measurements. There was a statistically significant effect of the bm-OTU pcDNA3.1 vector on these cells on early, late, and necrosis apoptosis levels.

The intracellular deubiquitinase activity of the bm-OTU recombinant protein was determined using the BML-PW8810-0500 antibody. The antibody only binds to ubiquitin-bound protein and has no effect on ubiquitin in its free form. The result showed smear bands due to its recognition property. The BML-PW8810 antibody was used to identify the mono-poly ubiquitination, and thus the amount of mono-poly-Ub protein increased remarkably in the presense of bm-OTU which illustrates the necessity of testing mono-Ub and poly-Ub separately.

Analysis of gene expression in HEK293 mammalian cells after transfection of bm-OTU pcDNA3.1 was performed to determine the effect on molecular responses, recognize molecular mechanisms of action, and control the expressed genes in the NF-κB pathway. The result shows the AIM2 gene from the pyroptosis pathway has an increase compared to the control; in contrast, the IL18 also from the pyroptosis pathway genes has an increase in the bmOTU-pcDNA3.1. There was no change in most cellular immune response genes; however, IFNAR1 and NFKB1 genes slightly decreased expression levels. Additionally, there was an overall decrease in interferon stimulatory genes STAT1, and IL15, while the expression of APOBEC3G and C1P2 reduced considerably. Lastly, most apoptotic genes remained unchanged, like BCL2L1, BCL2A1, and BID, but the expression of the BAK gene was dramatically increased, which means an overexpression of the gene. The outcome of this experimentation leads to conclude that bm-OTU deubiquitinase protein carries out its activity through the selected genes and pathways.

In conclusion, this study highlights the challenge of deubiquitination activity of the bm-OTU recombinant protein *in vitro* and accredits any improvements in different conditions. It can be drawn from all the results shown in this study that the studied recombinant protein has been identified and characterized for any future work in order to develop any new approaches in the field of treatments.

6. FUTURE DIRECTIONS

After the bmOTU protein has been transferred to BL21 cell line, mass produced, extracted, purified, and incubated with the ubiquitin substrate, the second step of the project which is determining the protease activity and small molecules candidates could be performed such as:

Following steps:

1. Using stablilizers during mass production in bacterial cells to avoid any modification of the protein.
2. Take the sample to mass spectroscopy for analyzing the recombinant protein.
3. Change the conditions of the DUB assay such as temperature and protein concentration.
4. Perform bioinformatics (Docking) to observe the avaliabity for developing new approaches as a treatment.

REFERENCES

1. Tick-Borne Diseases | NIOSH | CDC; [cited 2022 Mar 23]. Available from: https://www.cdc.gov/niosh/topics/tick-borne/default.html

2. Swanson M. Surveillance for Babesiosis. 2021 [cited 2022 Mar 23]. Available from: https://www.cdc.gov/parasites/babesiosis/resources/surveillance_babesiosis_us_2019.pdf.

3. Vannier E, Krause PJ. Update on Babesiosis. Interdisciplinary Perspectives on Infectious Diseases. 2009;2009:1–9.

4. Clark IA, Jacobson LS. Do babesiosis and malaria share a common disease process? *Annals of Tropical Medicine & Parasitology.* 1998 Jan;92(4):483–8.

5. Krause PJ, Telford SR, Ryan R, Conrad PA, Wilson M, Ohn J, et al. Diagnosis of Babesiosis: Evaluation of a Serologic Test for the Detection of Babesia microti Antibody 1994 [cited 2022 Mar 23]. Available from: http://jid.oxfordjournals.org/

6. Kjemtrup AM, Conrad PA. Human babesiosis: an emerging tick-borne disease; [cited 2022 Mar 23]. Available from: www.parasitology-online.com

7. Vannier E, Krause PJ. Babesiosis. In: Hunter's Tropical Medicine and Emerging Infectious Diseases Elsevier; 2020. p. 799–802 [cited 2022 Mar 24]. Available from: https://linkinghub.elsevier.com/retrieve/pii/B9780323555128001058

8. About Babesiosis; [cited 2022 Mar 24]. Available from: https://web.stanford.edu/group/parasites/ParaSites2002/babesiosis/aboutbab.html

9. Powell VI, Grima K. Exchange transfusion for malaria and babesia infection. *Transfusion Medicine Reviews.* 2002;16(3):239–50.

10. Western KA, Benson GD, Gleason NN, Healy GR, Schultz MG. Babesiosis in a Massachusetts Resident. *New England Journal of Medicine.* 1970 Oct 15;283(16):854–6.

11. Leiby DA. Transfusion-transmitted Babesia spp.: Bull's-eye on Babesia microti. *Clinical Microbiology Reviews.* 2011 Jan;24(1):14–28.

12. Leiby DA. Babesiosis and blood transfusion: Flying under the radar. *Vox Sanguinis*. 2006 Apr;90(3):157–65.

13. White DJ, Talarico J, Chang HG, Birkhead GS, Heimberger T, Morse DL. Human Babesiosis in New York State Review of 139 Hospitalized Cases and Analysis of Prognostic Factors; [cited 2022 Mar 25]. Available from: http://archinte.jamanetwork.com/

14. Hildebrandt A, Hunfeld KP, Baier M, Krumbholz A, Sachse S, Lorenzen T, et al. First confirmed autochthonous case of human Babesia microti infection in Europe. *European Journal of Clinical Microbiology and Infectious Diseases.* 2007 Aug;26(8):595–601.

15. Hildebrandt A, Gray JS, Hunfeld KP. Human Babesiosis in Europe: What clinicians need to know. Vol. 41, *Infection.* 2013. p. 1057–72.

16. Gray JS. Identity of the causal agents of human babesiosis in Europe. *International Journal of Medical Microbiology.* 2006;296(SUPPL. 1):131–6. Available from: www.elsevier.de/ijmm

17. Hunfeld KP, Hildebrandt A, Gray JS. Babesiosis: Recent insights into an ancient disease. *International Journal for Parasitology.* 2008 Sep;38(11):1219–37.

18. Zhou X, Xia S, Huang JL, Tambo E, Zhuge HX, Zhou XN. Human babesiosis, an emerging tick-borne disease in the People's Republic of China. 2014 [cited 2022 Mar 25];1–10. Available from: http://www.parasitesandvectors.com/content/7/1/509

19. Gray JS. Identity of the causal agents of human babesiosis in Europe. *International Journal of Medical Microbiology.* 2006 May 22;296(SUPPL. 1):131–6.

20. Yang Y, Christie J, Köster L, Du A, Yao C. Emerging Human Babesiosis with "Ground Zero" in North America. Microorganisms 2021, Vol 9, Page 440. 2021 Feb 20 [cited 2022 Mar 25];9(2):440. Available from: https://www.mdpi.com/2076-2607/9/2/440/htm

21. Krause PJ. Human babesiosis. Vol. 49, *International Journal for Parasitology.* Elsevier Ltd; 2019. p. 165–74.

22. Vannier EG, Diuk-Wasser MA, ben Mamoun C, Krause PJ. Babesiosis. Vol. 29, *Infectious Disease Clinics of North America.* W.B. Saunders; 2015. p. 357–70.

23. Hildebrandt A, Zintl A, Montero E, Hunfeld KP, Gray J. pathogens Human Babesiosis in Europe. 2021 [cited 2022 Mar 25]; Available from: https://doi.org/10.3390/pathogens10091165

24. Gorenflot A, Moubri K, Precigout E, Carcy B, Schetters TPM. Human babesiosis. In: Annals of Tropical Medicine and Parasitology. *Maney Publishing*; 1998. p. 489–501.

25. Gabrielli S, Calderini P, Cassini R, Galuppi R, Tampieri MP, Pietrobelli M, et al. Human exposure to piroplasms in Central and Northern Italy. Vet Ital. 2014 [cited 2022 Apr 6];50(1):41–7. Available from: https://pubmed.ncbi.nlm.nih.gov/24715592/

26. Rigaud E, Jaulhac B, Garcia-Bonnet N, Hunfeld KP, Féménia F, Huet D, et al. Seroprevalence of seven pathogens transmitted by the Ixodes ricinus tick in forestry workers in France. Clin Microbiol Infect. 2016 Aug 1 [cited 2022 Apr 6];22(8):735.e1-735.e9. Available from: https://pubmed.ncbi.nlm.nih.gov/27237545/

27. Svensson J, Hunfeld KP, Persson KEM. High seroprevalence of Babesia antibodies among Borrelia burgdorferi-infected humans in Sweden. Ticks Tick Borne Dis. 2019 Jan 1 [cited 2022 Apr 6];10(1):186–90. Available from: https://pubmed.ncbi.nlm.nih.gov/30389326/

28. Lempereur L, Shiels B, Heyman P, Moreau E, Saegerman C, Losson B, et al. A retrospective serological survey on human babesiosis in Belgium. Clin Microbiol Infect. 2015 [cited 2022 Apr 6];21(1):96.e1-96.e7. Available from: https://pubmed.ncbi.nlm.nih.gov/25636942/

29. Hildebrandt A, Zintl A, Montero E, Hunfeld KP, Gray J. Human babesiosis in europe. Vol. 10, *Pathogens.* MDPI; 2021.

30. González LM, Estrada K, Grande R, Jiménez-Jacinto V, Vega-Alvarado L, Sevilla E, et al. Comparative and functional genomics of the protozoan parasite Babesia divergens

highlighting the invasion and egress processes. PLoS Negl Trop Dis. 2019 [cited 2022 Apr 6];13(8). Available from: https://pubmed.ncbi.nlm.nih.gov/31425518/

31. Hyodo K, Okuno T. Hijacking of host cellular components as proviral factors by plant-infecting viruses. In: Advances in Virus Research. *Academic Press* Inc.; 2020.

32. Chen SC, Hung CC, Hsu CP, Chiu YW, Liu YC, Tsai JC, et al. Recurrent acute renal failure in a patient with aplastic anemia-paroxysmal nocturnal hemoglobinuria syndrome: A case report. *Kaohsiung Journal of Medical Sciences.* 2007;23(11):579–83.

33. Ozubek S, Bastos RG, Alzan HF, Inci A, Aktas M, Suarez CE. Bovine babesiosis in Turkey: Impact, current gaps, and opportunities for intervention. Vol. 9, *Pathogens.* MDPI AG; 2020. p. 1–23.

34. SKRABALO Z, DEANOVIC Z. Piroplasmosis in man; report of a case. Documenta de Medicina Geographica et Tropica. 1957 Mar 1 [cited 2022 Apr 16];9(1):11–6. Available from: http://europepmc.org/article/MED/13427667

35. The economics of integrated tick and tick-borne disease control on commercial farms in Zimbabwe; [cited 2022 Apr 16]. Available from: https://cgspace.cgiar.org/handle/10568/29964

36. Perkins ME. Rhoptry Organelles of Apicomplexan Parasites. Vol. 8, Parasitology Today. 1992.

37. Rudzinska MA, Spielman A, R I E K RF, Lewengrub SJ, D Joseph Piesman AN. Intraerythrocytic "gametocytes" of Babesia microti and their maturation in ticks1; [cited 2022 Mar 25]. Available from: www.nrcresearchpress.com

38. Wilson ML, Levine JF, Piesman J. ECOLOGY OF IXODES DAMMINI-BORNE HUMAN BABESIOSIS AND LYME DISEASE; [cited 2022 Mar 27]. Vol. 30, Ann. Rev. Entomol. 1985. Available from: www.annualreviews.org

39. Piesman J, Spielman A. Human babesiosis on Nantucket Island: prevalence of Babesia microti in ticks. Am J Trop Med Hyg 1980 [cited 2022 Apr 16];29(5). Available from: https://pubmed.ncbi.nlm.nih.gov/7435782/

40. Hedy G. The impact of cultural and environmental changes on the epidemiology and control of human babesiosis. Vol. 83. 1989.

41. Wei Q, Tsuji M, Zamoto A, Kohsaki M, Matsui T, Shiota T, et al. Human babesiosis in Japan: Isolation of Babesia microti-like parasites from an asymptomatic transfusion donor and from a rodent from an area where babesiosis is endemic. *Journal of Clinical Microbiology.* 2001;39(6):2178–83.

42. Krause PJ, Mckay K, Gadbaw J, Christianson D, Closter L, Lepore T, et al. INCREASING HEALTH BURDEN OF HUMAN BABESIOSIS IN ENDEMIC SITES. 2003.

43. Ruebush Ii TK, Cassaday PB, Marsh HJ, Lisker SA, Voorhees DB, Mahoney EB, et al. Human Babesiosis on Nantucket Island Clinical Features; [cited 2022 Mar 27] Available from: http://annals.org/pdfaccess.ashx?url=/data/journals/aim/19517/

44. White DJ, Talarico J, Chang HG, Birkhead GS, Heimberger T, Morse DL. Human Babesiosis in New York State Review of 139 Hospitalized Cases and Analysis of Prognostic Factors; [cited 2022 Apr 16]. Available from: http://archinte.jamanetwork.com/

45. Krause PJ. Concurrent Lyme Disease and Babesiosis. JAMA. 1996 Jun 5;275(21):1657.

46. Hatcher JC, Greenberg PD, Antique J, Jimenez-Lucho VE. Severe Babesiosis in Long Island: Review of 34 Cases and Their Complications; Severe Babesiosis in Long Island • CID. 2001 [cited 2022 Apr 16]. Available from: http://cid.oxfordjournals.org/

47. Life Cycle and Players; [cited 2022 Apr 16]. Available from: https://web.stanford.edu/group/parasites/ParaSites2002/babesiosis/lifeplay.html

48. Tomčala A, Michálek J, Schneedorferová I, Füssy Z, Gruber A, Vancová M, et al. Fatty acid biosynthesis in chromerids. *Biomolecules.* 2020 Aug 1;10(8):1–26.

49. Clark IA, Budd AC, Hsue G, Haymore BR, Joyce AJ, Thorner R, et al. Absence of erythrocyte sequestration in a case of babesiosis in a splenectomized human patient. *Malaria Journal.* 2006 Aug 4;5.

50. O'connor RM, Lane TJ, Stroup SE, Allred DR. Characterization of a variant erythrocyte surface antigen (VESA1) expressed by Babesia bo6is during antigenic variation. Vol. 89, *Molecular and Biochemical Parasitology.* 1997.

51. Aguilar-Delfin I, Wettstein PJ, Persing DH. Resistance to acute babesiosis is associated with interleukin-12- and gamma interferon-mediated responses and requires macrophages and natural killer cells. *Infection and Immunity.* 2003 Apr 1;71(4):2002–8.

52. Wood PR, Clark IA. Apparent irrelevance of NK cells to resolution of infections with Babesia microti and Plasmodium vinckei petteri in mice. Vol. 4, *Parasite Immunology.* 1982.

53. Goff WL, Johnson WC, Parish SM, Barrington GM, Elsasser TH, Davis WC, et al. IL-4 and IL-10 inhibition of IFN-g-and TNF-a-dependent nitric oxide production from bovine mononuclear phagocytes exposed to Babesia bovis merozoites.

54. Clark IA, Alleva LM, Mills AC, Cowden WB. Pathogenesis of malaria and clinically similar conditions. Vol. 17, Clinical Microbiology Reviews. *American Society for Microbiology;* 2004. p. 509–39.

55. Capodagli GC, Deaton MK, Baker EA, Lumpkin RJ, Pegan SD. Diversity of Ubiquitin and ISG15 Specificity among Nairoviruses' Viral Ovarian Tumor Domain Proteases. *Journal of Virology.* 2013 Apr;87(7):3815–27.

56. Akutsu M, Ye Y, Virdee S, Chin JW, Komander D. Molecular basis for ubiquitin and ISG15 cross-reactivity in viral ovarian tumor domains; [cited 2022 Jun 5]. Available from: www.pymol.org

57. Chiuya T, Masiga DK, Falzon LC, Bastos ADS, Fèvre EM, Villinger J. Tick-borne pathogens, including Crimean-Congo haemorrhagic fever virus, at livestock markets and slaughterhouses in western Kenya. *Transboundary and Emerging Diseases.* 2021 Jul 1;68(4):2429–45.

58. Kocabas F, Aslan GS. Fluorometric CCHFV OTU protease assay with potent inhibitors. *Virus Genes.* 2015 Oct 23;51(2):190–7.

59. Dai S, Deng F, Wang H, Ning Y. Crimean-Congo hemorrhagic fever virus: Current advances and future prospects of antiviral strategies. *Viruses.* 2021 Jul 1;13(7).

60. Bergeron É, Albariño CG, Khristova ML, Nichol ST. Crimean-Congo Hemorrhagic Fever Virus-Encoded Ovarian Tumor Protease Activity Is Dispensable for Virus RNA Polymerase Function. *Journal of Virology.* 2010 Jan;84(1):216–26.

61. Kocabas F, Aslan GS. Fluorometric CCHFV OTU protease assay with potent inhibitors. *Virus Genes.* 2015 Oct 23;51(2):190–7.

62. Papadopoulos JS, Agarwala R. COBALT: constraint-based alignment tool for multiple protein sequences. Bioinformatics 2007 May [cited 2022 Jun 5];23(9):1073–9. Available from: https://pubmed.ncbi.nlm.nih.gov/17332019/

63. Kocabaş F, Ergin EK. Identification of small molecule binding pocket for inhibition of crimean–congo hemorrhagic fever virus OTU protease. *Turkish Journal of Biology.* 2016;40(1):239–49.

64. Wang J, Gao S, Zhang S, He X, Liu J, Liu A, et al. Rapid detection of Babesia motasi responsible for human babesiosis by cross-priming amplification combined with a vertical flow. *Parasites and Vectors.* 2020 Jul 29;13(1).

65. Scott JD, Sajid MS, Pascoe EL, Foley JE. Detection of babesia odocoilei in humans with babesiosis symptoms. *Diagnostics.* 2021 Jun 1;11(6).

66. Krause PJ, Mckay K, Thompson CA, Sikand VK, Lentz R, Lepore T, et al. Disease-Specific Diagnosis of Coinfecting Tickborne Zoonoses: Babesiosis, Human Granulocytic Ehrlichiosis, and Lyme Disease 2002 [cited 2022 Jun 6]. Available from: http://cid.oxfordjournals.org/

67. Vannier E, Gewurz BE, Krause PJ. Human Babesiosis. Vol. 22, I*nfectious Disease Clinics of North America.* 2008. p. 469–88.

68. Eter K Rause PJ, Imothy Epore TL, Ijay S Ikand VK, Oseph Adbaw JG, Eorgine Urke GB, R T Elford Iii SA, et al. The New Eng land Jour nal of Medicine ATOVAQUONE AND AZITHROMYCIN FOR THE TREATMENT OF BABESIOSIS A BSTRACT. 2000.

69. Wormser GP, Dattwyler RJ, Shapiro ED, Halperin JJ, Steere AC, Klempner MS, et al. The Clinical Assessment, Treatment, and Prevention of Lyme Disease, Human Granulocytic Anaplasmosis, and Babesiosis: Clinical Practice Guidelines by the Infectious Diseases Society of America 2006 [cited 2022 Jun 6]. Available from: http://cid.oxfordjournals.org/

70. Vyas JM, Telford SR, Robbins GK. Treatment of refractory Babesia microti infection with atovaquone-proguanil in an HIV-infected patient: Case report. *Clinical Infectious Diseases.* 2007 Dec 15;45(12):1588–90.

71. Krause PJ, Gewurz BE, Hill D, Marty FM, Vannier E, Foppa IM, et al. Persistent and relapsing babesiosis in immunocompromised patients. *Clinical Infectious Diseases.* 2008 Feb 1;46(3):370–6.

72. Florin-Christensen M, Wieser SN, Suarez CE, Schnittger L. In silico survey and characterization of babesia microti functional and non-functional proteases. *Pathogens.* 2021 Nov 1;10(11).

73. Ciechanover A, Schwartz AL. The ubiquitin-proteasome pathway: The complexity and myriad functions of proteins death; Vol. 95. 1998 [cited 2022 Apr 29]. Available from: www.pnas.org.

74. Saeki Y. JB special review - Recent topics in ubiquitin-proteasome system and autophagy: Ubiquitin recognition by the proteasome. Vol. 161, *Journal of Biochemistry*. Oxford University Press; 2017. p. 113–24.

75. Lecker SH, Goldberg AL, Mitch WE. Protein degradation by the ubiquitin-proteasome pathway in normal and disease states. Vol. 17, *Journal of the American Society of Nephrology*. 2006. p. 1807–19.

76. Wilson ML, Iii SRT, Piesman J, Spielman A. Reduced Abundance of Immature Ixodes dammini (Acari: Ixodidae) Following Elimination of Deer. Vol. 25, J. Med. Entomol. 1988 [cited 2022 Jun 8]. Available from: http://jme.oxfordjournals.org/

77. CDC - Babesiosis - Biology; [cited 2022 Jun 8]. Available from: https://www.cdc.gov/parasites/babesiosis/biology.html

78. Papa A, Tsergouli K, Tsioka K, Mirazimi A. Crimean-Congo hemorrhagic fever: Tick-host-virus interactions. Vol. 7, *Frontiers in Cellular and Infection Microbiology*. Frontiers Media S.A.; 2017.

79. Kocabas F, Aslan GS. Fluorometric CCHFV OTU protease assay with potent inhibitors. *Virus Genes.* 2015 Oct 23;51(2):190–7.

80. NCBI Conserved Domain Search; [cited 2022 Jun 8]. Available from: https://www.ncbi.nlm.nih.gov/Structure/cdd/wrpsb.cgi

81. Siyah P, Akgol S, Durdagi S, Kocabas F. Identification of first-in-class plasmodium OTU inhibitors with potent anti-malarial activity. Biochem J 2021 Sep 1 [cited 2022 Jun 8];478(18):3445–66. Available from: https://pubmed.ncbi.nlm.nih.gov/34486667/

82. Asghari S, Khaniani MS, Darabi M, Derakhshan SM. Cloning of soluble human stem cell factor in pET-26b(+) vector. *Advanced Pharmaceutical Bulletin.* 2014;4(1):91–5.

83. Skretas G, Ventura S. Editorial: Protein Aggregation and Solubility in Microorganisms (Archaea, Bacteria and Unicellular Eukaryotes): Implications and Applications. Vol. 11, *Frontiers in Microbiology.* Frontiers Media S.A.; 2020.

84. Trevino SR, Scholtz JM, Pace CN. Measuring and increasing protein solubility. Vol. 97, *Journal of Pharmaceutical Sciences.* John Wiley and Sons Inc.; 2008. p. 4155–66.

85. Dumont J, Euwart D, Mei B, Estes S, Kshirsagar R. Human cell lines for biopharmaceutical manufacturing: history, status, and future perspectives. *Critical Reviews in Biotechnology.* 2016 Nov 1;36(6):1110–22.

86. Longo PA, Kavran JM, Kim MS, Leahy DJ. Transient Mammalian Cell Transfection with Polyethylenimine (PEI). Methods Enzymol 2013 [cited 2022 Jun 9];529:227. Available from: /pmc/articles/PMC4012321/

87. Waterhouse A, Bertoni M, Bienert S, Studer G, Tauriello G, Gumienny R, et al. SWISS-MODEL: Homology modelling of protein structures and complexes. *Nucleic Acids Research.* 2018 Jul 2;46(W1):W296–303.

APPENDIX A

BIOZENTRUM
University of Basel
The Center for Molecular Life Sciences

SWISS-MODEL Homology Modelling Report

Model Building Report

This document lists the results for the homology modelling project "bmotu" submitted to SWISS-MODEL workspace on June 15, 2022, 11:03 a.m..The submitted primary amino acid sequence is given in Table T1.

If you use any results in your research, please cite the relevant publications:

- Waterhouse, A., Bertoni, M., Bienert, S., Studer, G., Tauriello, G., Gumienny, R., Heer, F.T., de Beer, T.A.P., Rempfer, C., Bordoli, L., Lepore, R., Schwede, T. SWISS-MODEL: homology modelling of protein structures and complexes. Nucleic Acids Res. 46(W1), W296-W303 (2018). doi
- Bienert, S., Waterhouse, A., de Beer, T.A.P., Tauriello, G., Studer, G., Bordoli, L., Schwede, T. The SWISS-MODEL Repository - new features and functionality. Nucleic Acids Res. 45, D313-D319 (2017). doi
- Studer, G., Tauriello, G., Bienert, S., Biasini, M., Johner, N., Schwede, T. ProMod3 - A versatile homology modelling toolbox. PLOS Comp. Biol. 17(1), e1008667 (2021). doi
- Studer, G., Rempfer, C., Waterhouse, A.M., Gumienny, G., Haas, J., Schwede, T. QMEANDisCo - distance constraints applied on model quality estimation. Bioinformatics 36, 1765-1771 (2020). doi
- Bertoni, M., Kiefer, F., Biasini, M., Bordoli, L., Schwede, T. Modeling protein quaternary structure of homo- and hetero-oligomers beyond binary interactions by homology. Scientific Reports 7 (2017). doi

Results

The SWISS-MODEL template library (SMTL version 2022-06-08, PDB release 2022-06-03) was searched with BLAST (Camacho et al.) and HHblits (Steinegger et al.) for evolutionary related structures matching the target sequence in Table T1. For details on the template search, see Materials and Methods. Overall 142 templates were found (Table T2).

Models

The following model was built (see Materials and Methods "Model Building"):

Model #01	File	Built with	Oligo-State	Ligands	GMQE	QMEANDisCo Global
	PDB	ProMod3 3.2.1	monomer (matching prediction)	None	0.55	0.67 ± 0.07

Template	Seq Identity	Oligo-state	QSQE	Found by	Method	Resolution	Seq Similarity	Range	Coverage	Description
4bop.1.A	28.28	homo-octamer	0.07	HHblits	X-ray	2.10Å	0.33	41 - 191	0.76	OTU DOMAIN-CONTAINING PROTEIN 1

Excluded ligands

Ligand Name.Number	Reason for Exclusion	Description
PO4.1	Not biologically relevant.	PHOSPHATE ION
PO4.2	Not biologically relevant.	PHOSPHATE ION
PO4.3	Not biologically relevant.	PHOSPHATE ION
PO4.4	Not biologically relevant.	PHOSPHATE ION
PO4.5	Not biologically relevant.	PHOSPHATE ION
PO4.6	Not biologically relevant.	PHOSPHATE ION
PO4.7	Not biologically relevant.	PHOSPHATE ION
PO4.8	Not biologically relevant.	PHOSPHATE ION

```
Target    MEGFYTNKPLTCSQKKKLKKKQQQLQIDIEKDAVKSTDTSKSQEERALDIQLAIYGFRIYNIPGDGNCLYRSIAHQLDPK
4bop.1.A  ----------------------------------------YLAEVEKQDKYLRQRNKYRFHIIPDGNCLYRAVSKTVYG-
```


Figure A.1. Homology modelling of bmOTU protein report [87]

```
Target    STELHRELRVKAAKFILDHREEFSSYISDNICEYADKIANTNEWGGEIEIVALSRALNRNIFVHCVRYKEPICHVKIMIM
4bop.1.A  DQSLHRELREQTVHYIADHLDHFSPLIEGDVGEFIIAAAQDGAWAGYPELLAMGQMLNVNIHLTTGGRLESPTVSTMIHY

Target    QGHTSAVGDDIHLVFYESAYLLGGHYNSVTKL
4bop.1.A  LGPEDSLRPSIWLSWL-----SNGHYDAVFD-
```

Materials and Methods

Template Search

Template search with BLAST and HHblits has been performed against the SWISS-MODEL template library (SMTL, last update: 2022-06-08, last included PDB release: 2022-06-03).

The target sequence was searched with BLAST against the primary amino acid sequence contained in the SMTL. A total of 27 templates were found.

An initial HHblits profile has been built using the procedure outlined in (Steinegger et al.), followed by 1 iteration of HHblits against Uniclust30 (Mirdita, von den Driesch et al.). The obtained profile has then be searched against all profiles of the SMTL. A total of 140 templates were found.

Template Selection

For each identified template, the template's quality has been predicted from features of the target-template alignment. The templates with the highest quality have then been selected for model building.

Model Building

Models are built based on the target-template alignment using ProMod3 (Studer et al.). Coordinates which are conserved between the target and the template are copied from the template to the model. Insertions and deletions are remodelled using a fragment library. Side chains are then rebuilt. Finally, the geometry of the resulting model is regularized by using a force field.

Model Quality Estimation

The global and per-residue model quality has been assessed using the QMEAN scoring function (Studer et al.).

Ligand Modelling

Ligands present in the template structure are transferred by homology to the model when the following criteria are met: (a) The ligands are annotated as biologically relevant in the template library, (b) the ligand is in contact with the model, (c) the ligand is not clashing with the protein, (d) the residues in contact with the ligand are conserved between the target and the template. If any of these four criteria is not satisfied, a certain ligand will not be included in the model. The model summary includes information on why and which ligand has not been included.

Oligomeric State Conservation

The quaternary structure annotation of the template is used to model the target sequence in its oligomeric form. The method (Bertoni et al.) is based on a supervised machine learning algorithm, Support Vector Machines (SVM), which combines interface conservation, structural clustering, and other template features to provide a quaternary structure quality estimate (QSQE). The QSQE score is a number between 0 and 1, reflecting the expected accuracy of the interchain contacts for a model built based a given alignment and template. Higher numbers indicate higher reliability. This complements the GMQE score which estimates the accuracy of the tertiary structure of the resulting model.

References

- **BLAST**
  Camacho, C., Coulouris, G., Avagyan, V., Ma, N., Papadopoulos, J., Bealer, K., Madden, T.L. BLAST+: architecture and applications. BMC Bioinformatics 10, 421-430 (2009). doi
- **HHblits**
  Steinegger, M., Meier, M., Mirdita, M., Vöhringer, H., Haunsberger, S. J., Söding, J. HH-suite3 for fast remote homology detection and deep protein annotation. BMC Bioinformatics 20, 473 (2019). doi

- **Uniclust30**
  Mirdita, M., von den Driesch, L., Galiez, C., Martin, M.J., Söding, J., Steinegger, M. Uniclust databases of clustered and deeply annotated protein sequences and alignments. Nucleic Acids Research 45, D170–D176 (2016). doi>

Table T1:

Primary amino acid sequence for which templates were searched and models were built.

```
MEGFYTNKPLTCSQKKKLKKKQQQLQIDIEKDAVKSTDTSKSQEERALDIQLAIYGFRIYNIPGDGNCLYRSIAHQLDPKSTELHRELRVKAAKFILDHR
EEFSSYISDNICEYADKIANTNEWGGEIEIVALSRALNRNIFVHCVRYKEPICHVKIMIMQGHTSAVGDDIHLVFYESAYLLGGHYNSVTKL
```

Table T2:

Template	Seq Identity	Oligo-state	QSQE	Found by	Method	Resolution	Seq Similarity	Coverage	Description
4bop.1.A	28.28	homo-octamer	0.07	HHblits	X-ray	2.10Å	0.33	0.76	OTU DOMAIN-CONTAINING PROTEIN 1
3tmp.2.A	23.61	monomer	-	HHblits	X-ray	1.91Å	0.33	0.75	OTU domain-containing protein 5
3tmp.1.A	23.61	monomer	-	HHblits	X-ray	1.91Å	0.33	0.75	OTU domain-containing protein 5
4bou.1.A	27.41	homo-dimer	0.22	HHblits	X-ray	1.55Å	0.36	0.70	OTU DOMAIN-CONTAINING PROTEIN 3
4bou.1.A	30.23	homo-dimer	0.20	BLAST	X-ray	1.55Å	0.38	0.67	OTU DOMAIN-CONTAINING PROTEIN 3
3pfy.1.A	26.06	monomer	-	HHblits	X-ray	1.70Å	0.34	0.74	OTU domain-containing protein 5
3tmo.1.A	23.61	monomer	-	HHblits	X-ray	2.20Å	0.33	0.75	OTU domain-containing protein 5
6dx2.1.A	23.85	monomer	-	HHblits	X-ray	1.61Å	0.31	0.68	RNA-dependent RNA polymerase
3znh.1.A	20.59	monomer	-	HHblits	X-ray	2.30Å	0.31	0.71	UBIQUITIN THIOESTERASE
5v5g.2.A	20.59	monomer	-	HHblits	X-ray	2.10Å	0.31	0.71	RNA-directed RNA polymerase L
5v5g.1.A	20.59	monomer	-	HHblits	X-ray	2.10Å	0.31	0.71	RNA-directed RNA polymerase L
3pse.1.A	20.59	monomer	-	HHblits	X-ray	2.30Å	0.31	0.71	RNA polymerase
3prm.1.A	20.90	monomer	-	HHblits	X-ray	2.30Å	0.31	0.70	L protein
3prp.2.A	20.90	monomer	-	HHblits	X-ray	1.70Å	0.31	0.70	L protein
3phw.1.A	20.59	monomer	-	HHblits	X-ray	2.00Å	0.31	0.71	RNA-directed RNA polymerase L
6oat.1.A	23.31	monomer	-	HHblits	X-ray	3.17Å	0.31	0.69	RNA-dependent RNA polymerase
3phx.1.A	20.59	monomer	-	HHblits	X-ray	1.60Å	0.31	0.71	RNA-directed RNA polymerase L
4bop.1.A	34.40	homo-octamer	0.07	BLAST	X-ray	2.10Å	0.38	0.65	OTU DOMAIN-CONTAINING PROTEIN 1
6dwx.2.A	18.90	monomer	-	HHblits	X-ray	2.39Å	0.29	0.66	RNA-dependent RNA polymerase
7jms.2.A	27.69	monomer	-	HHblits	X-ray	2.78Å	0.33	0.68	Replicase
7jms.4.A	27.69	monomer	-	HHblits	X-ray	2.78Å	0.33	0.68	Replicase
6dwx.1.A	18.90	monomer	-	HHblits	X-ray	2.39Å	0.29	0.66	RNA-dependent RNA polymerase
7jms.1.A	27.69	monomer	-	HHblits	X-ray	2.78Å	0.33	0.68	Replicase
6dx3.1.A	18.60	monomer	-	HHblits	X-ray	2.05Å	0.31	0.67	RNA-dependent RNA polymerase
4bos.1.B	23.58	homo-dimer	0.16	HHblits	X-ray	2.35Å	0.31	0.64	UBIQUITIN THIOESTERASE OTU1

Template	Seq Identity	Oligo-state	QSQE	Found by	Method	Resolution	Seq Similarity	Coverage	Description
7jms.3.A	27.69	monomer	-	HHblits	X-ray	2.78Å	0.33	0.68	Replicase
6dx5.1.A	20.77	homo-dimer	0.10	HHblits	X-ray	2.22Å	0.31	0.68	RNA-dependent RNA polymerase
6dx5.1.B	20.77	homo-dimer	0.10	HHblits	X-ray	2.22Å	0.31	0.68	RNA-dependent RNA polymerase
3c0r.2.A	25.98	monomer	-	HHblits	X-ray	2.32Å	0.32	0.66	Ubiquitin thioesterase OTU1
4bos.1.A	23.58	homo-dimer	0.16	HHblits	X-ray	2.35Å	0.31	0.64	UBIQUITIN THIOESTERASE OTU1
5jze.1.B	21.71	monomer	-	HHblits	X-ray	2.47Å	0.30	0.67	RNA-dependent RNA polymerase
4boz.1.A	23.02	monomer	-	HHblits	X-ray	3.03Å	0.31	0.66	UBIQUITIN THIOESTERASE OTU1
3by4.1.A	25.98	monomer	-	HHblits	X-ray	1.55Å	0.32	0.66	Ubiquitin thioesterase OTU1
4hxd.1.B	24.43	monomer	-	HHblits	X-ray	2.85Å	0.32	0.68	RNA-directed RNA polymerase L
6oar.1.A	25.38	monomer	-	HHblits	X-ray	2.06Å	0.31	0.68	RNA-dependent RNA polymerase
4boq.1.A	23.20	homo-dimer	0.02	HHblits	X-ray	1.47Å	0.31	0.65	UBIQUITIN THIOESTERASE OTU1
6w9r.1.B	15.50	monomer	-	HHblits	X-ray	1.82Å	0.29	0.67	OTU domain-containing protein wMelOTU
6oar.1.A	33.33	monomer	-	BLAST	X-ray	2.06Å	0.36	0.59	RNA-dependent RNA polymerase
4ldt.1.A	16.33	monomer	-	HHblits	X-ray	1.90Å	0.30	0.51	Ubiquitin thioesterase otubain-like
4dhj.1.A	16.49	monomer	-	HHblits	X-ray	2.35Å	0.31	0.51	Ubiquitin thioesterase otubain-like
4hxd.1.B	32.46	monomer	-	BLAST	X-ray	2.85Å	0.36	0.59	RNA-directed RNA polymerase L
4dhi.1.A	16.49	monomer	-	HHblits	X-ray	1.80Å	0.31	0.51	Ubiquitin thioesterase otubain-like
3pfy.1.A	28.42	monomer	-	BLAST	X-ray	1.70Å	0.36	0.49	OTU domain-containing protein 5
4dhj.2.A	16.49	monomer	-	HHblits	X-ray	2.35Å	0.31	0.51	Ubiquitin thioesterase otubain-like
4dhj.5.A	16.49	monomer	-	HHblits	X-ray	2.35Å	0.31	0.51	Ubiquitin thioesterase otubain-like
6w9o.1.A	18.52	monomer	-	HHblits	X-ray	1.47Å	0.30	0.56	OTU domain-containing protein wMelOTU
7jms.1.A	34.09	monomer	-	BLAST	X-ray	2.78Å	0.38	0.46	Replicase
7jms.2.A	34.09	monomer	-	BLAST	X-ray	2.78Å	0.38	0.46	Replicase
6dx3.1.A	37.86	monomer	-	BLAST	X-ray	2.05Å	0.38	0.54	RNA-dependent RNA polymerase
7jms.3.A	34.09	monomer	-	BLAST	X-ray	2.78Å	0.38	0.46	Replicase

The table above shows the top 50 filtered templates. A further 84 templates were found which were considered to be less suitable for modelling than the filtered list.
1tff.1.A, 2jn4.1.A, 2lyy.1.A, 2lyy.1.B, 2vfj.1.A, 2zfy.1.A, 3dkb.1.A, 3dkb.4.A, 3fyf.1.A, 3fyf.1.B, 3phu.1.A, 3phu.2.A, 3phw.1.A, 3phx.1.A, 3prm.1.A, 3prp.2.A, 3pse.1.A, 3pt2.1.A, 3tmo.1.A, 3tmp.1.A, 3tmp.2.A, 3von.1.A, 3zjd.1.A, 3zjd.1.B, 3znh.1.A, 3znv.1.A, 3znx.1.A, 3znz.1.A, 3zrh.1.A, 4a5u.1.A, 4ddg.1.A, 4ddg.1.C, 4fjv.1.A, 4gdz.1.A, 4i6l.1.A, 4ksj.1.A, 4ksk.1.A, 4ksl.1.A, 4ksl.6.A, 4rou.1.A, 5bz0.1.A, 5dq6.1.A, 5dq6.2.A, 5lru.1.A, 5lrv.1.A, 5lrw.1.A, 5lrx.2.A, 5lrx.4.A, 5lw5.1.A, 5lwa.1.A, 5lwa.2.A, 5oe7.1.A, 5oql.1.2, 5qio.1.A, 5qip.1.A, 5v3b.2.A, 5v3p.1.A, 5v3p.3.A, 5v3p.3.B, 5v5g.1.A, 5v5g.2.A, 5v5h.1.A, 5v5i.1.A, 6i9c.1.A, 6k9n.1.A, 6k9p.1.A, 6ks5.1.A, 6ks5.2.A, 6ln0.1.A, 6oat.1.A, 6rxt.1.2, 6rxy.1.2, 6rxz.29.A, 6sak.1.A, 6w9s.1.A, 6yk8.1.A, 6ypt.1.A, 7bu0.1.A, 7bu0.1.B, 7f9x.1.A, 7jms.4.A, 7mia.1.A, 7mia.2.A, 7mic.1.A

Figure A.2. Multiple alignment of the CCHFV OTU protease-related proteins [63]